Evaluation of bedload transport predictions using flow resistance equations to account for macro-roughness in steep mountain streams

Manuel Nitsche,[1] Dieter Rickenmann,[1] Jens M. Turowski,[1] Alexandre Badoux,[1] and James W. Kirchner[1]

Received 9 March 2011; revised 10 June 2011; accepted 16 June 2011; published 16 August 2011.

[1] Steep mountain streams typically feature macro-roughness elements like boulders, step-pool sequences, and a varying channel width. Flow resistance because of such roughness elements appears to be an important control on bedload transport rates. Many commonly used bedload transport equations overestimate the transport in steep streams by orders of magnitude. Few approaches take into account the typical macro-roughness elements, and systematic tests of these models with field observations are lacking. In the present study several approaches were considered that allow calculating the contribution of macro-roughness elements to flow resistance. These approaches were combined with bedload transport equations and the predictions were compared to field measurements of discharge, transported bedload volumes, and channel characteristics in 13 Swiss mountain streams. The streams have channel slopes ranging from 2% to 19%, and catchment areas of 0.5 to 170 km^2. For six streams there were time series of sediment yields, mostly measured annually, and for the other seven streams sediment volume estimates were available for large flood events in 2000 and 2005. All tested equation combinations achieved an improvement in bedload prediction compared to a reference equation that was uncorrected for macro-roughness. The prediction accuracy mainly depended on the size and density of the macro-roughness and on flow conditions. The best performance overall was achieved by an empirical approach accounting for macro-roughness, on the basis of an independent data set of flow resistance measurements.

Citation: Nitsche, M., D. Rickenmann, J. M. Turowski, A. Badoux, and J. W. Kirchner (2011), Evaluation of bedload transport predictions using flow resistance equations to account for macro-roughness in steep mountain streams, *Water Resour. Res., 47*, W08513, doi:10.1029/2011WR010645.

1. Introduction

[2] In densely populated areas like the European Alps, bedload movement during floods is a frequent natural hazard. Using data from the Swiss flood and landslide damage database [*Hilker et al.*, 2009], we estimated that one third to one half of the total damage, at a cost of three billion Swiss francs, was associated with sediment transport processes during the large storm events of 2005 in Switzerland. To prevent or reduce this damage, it is of great importance to be able to accurately predict bedload transport rates. However, conventional transport equations typically overestimate bedload volumes in steep mountain streams by up to three orders of magnitude [e.g., *Bathurst et al.*, 1987; *Chiari and Rickenmann*, 2011; *Lenzi et al.*, 1999; *Rickenmann*, 2001]. One possible reason for this is that many equations were developed and calibrated with data from flume experiments or low gradient streams, with channel bed and transport characteristics that differ from those in steep mountain streams.

[3] Typically, steep streams with channel slopes above 5% feature (1) wide-grain size distributions, (2) large boulders that remain immobile during most floods, (3) channel-spanning bedforms such as step-pool morphologies, (4) shallow flows, and (5) variable channel widths. The channel bed tends to organize into patches or clusters of similar grain sizes [e.g., *Lamarre and Roy*, 2008; *Yager*, 2006], or steps spanning the width of the channel develop around large grains [e.g., *Church and Zimmermann*, 2007; *Whittaker and Jaeggi*, 1982; *Zimmermann et al.*, 2008]. These features lead to additional roughness and flow resistance that are absent in lower-gradient channels, and are rarely taken into account in laboratory investigations.

[4] Macro-roughness elements are physical sources of flow resistance. Boulders sitting in a bed of finer material disrupt the flow and increase turbulence [e.g., *Bathurst*, 1978; *Canovaro et al.*, 2007; *Papanicolaou et al.*, 2004; *Wohl and Thompson*, 2000; *Yager et al.*, 2007]. Jets of critical or supercritical flow originate at steps and plunge into downstream pools, where velocity decreases abruptly and hydraulic jumps, roller eddies, and substantial turbulence result [e.g., *Nelson et al.*, 1993; *Wilcox et al.*, 2006; *Wilcox*

[1]Mountain Hydrology and Torrents Unit, WSL Swiss Federal Institute for Forest, Snow and Avalanche Research SLF, Birmensdorf, Switzerland.

0043-1397/11/2011WR010645

and Wohl, 2007; *Wohl and Thompson*, 2000]. *Zimmermann* [2010] concluded that a major part of the flow energy in steep streams is dissipated by form and spill drag around roughness elements like step-pools. The contribution of these structures to total flow resistance increases with decreasing relative submergence of the bed.

[5] Several authors have proposed resistance equations specifically for shallow flows in mountain streams [*Bathurst*, 1978, 1985, 2002; *Jarrett*, 1984; *Katul et al.*, 2002; *Rickenmann*, 1991; *Smart et al.*, 2002]. Some have derived empirical flow resistance equations from velocity measurements in gravel and boulder bed streams [*Bathurst*, 1978; *Ferguson*, 2007; *Hey*, 1979; *Rickenmann and Recking*, 2011]. In most of these approaches the friction factor may be described as a function of the relative submergence d/D, where d is the average flow depth, and D is a representative grain size. However, it has been shown for some mountain streams with very pronounced step-pool structures that, for example, channel type and unit discharge are factors that might better predict flow resistance than d/D [*Comiti et al.*, 2009; *David et al.* 2010]. Few approaches directly include a measure of boulders or steps to account for macro-roughness in the flow resistance equations [*Canovaro and Solari*, 2007; *Egashira and Ashida*, 1991; *Pagliara and Chiavaccini*, 2006; *Papanicolaou et al.*, 2004; *Whittaker*, 1986; *Whittaker et al.*, 1988; *Yager*, 2006; *Yager et al.*, 2007]. Moreover, none of the latter mechanistic approaches has been validated for a wide range of natural conditions and systematically tested with field observations.

[6] The importance of accounting for additional energy losses (or increased total flow resistance) in steep streams in the context of bedload transport calculations was pointed out in several contributions [*Chiari and Rickenmann*, 2011; *Govers and Rauws*, 1986; *Palt*, 2001; *Rickenmann*, 2001, 2005; *Rickenmann and Koschni*, 2010; *Yager et al.*, 2007; *Zimmermann*, 2010]. In some of these studies, concepts similar to the grain and form resistance partitioning in lowland rivers were also applied in steep streams with some success. Flow resistance partitioning has been found to be particularly important for flow conditions with intermediate and large-scale roughness [*Rickenmann and Recking*, 2011], as compared to small-scale roughness conditions [sensu *Bathurst et al.*, 1981] with deeper flows for which most bedload transport equations were developed.

[7] In the present study, we tested how the use of different flow resistance equations affect predictions of bedload volumes transported in mountain streams. Four out of five tested equations for flow resistance explicitly include a measure of macro-roughness, while one approach is based on an empirical relationship that depends mainly on relative flow depth.

[8] Flow resistance partitioning was used to estimate the flow energy available for bedload transport. The reduced energy due to the macro-roughness was accounted for in the bedload transport equations by reducing the energy slope. The results of the bedload transport predictions were tested against field observations of bedload transport from 13 Swiss mountain streams. In six of the streams, bedload volumes were regularly measured for several decades using retention basins located near discharge gages. In the remaining seven streams, bedload volumes transported in a single extreme event were estimated in the field. The systematic evaluation of flow resistance partitioning approaches permits an assessment of their suitability for bedload transport prediction in steep natural mountain streams. Their suitability with regard to the type of dominant bed morphology and problems of parameter identification in the field are also discussed.

2. Flow Resistance and Bedload Transport Equations

[9] Total flow resistance in streams is typically defined with a roughness or friction parameter, namely Manning's n, the Darcy-Weisbach friction factor f, or the Chezy coefficient C. These are related by

$$v = C\sqrt{dS} = \sqrt{\frac{8gdS}{f}} = \frac{d^{2/3}\sqrt{S}}{n}. \quad (1)$$

[10] Here, v = depth-averaged flow velocity, S = friction slope which is often approximated by the water surface slope or the channel bed slope (for steady uniform flow in a prismatic channel), and g = acceleration due to gravity. The friction factor f is preferable over C or n, because it is a nondimensional quantity that can be physically interpreted as a drag coefficient [*Ferguson*, 2007]. It will therefore be used throughout this study.

[11] Published equations to calculate flow resistance and bedload transport include approaches that explicitly account for the effects of large roughness elements. The flow resistance approaches described here were applied to natural streambeds, with the simplifying assumption that the streambed is composed of a heterogeneous combination of finer base material and larger roughness elements like boulders and steps. In the literature the total resistance is often written as the sum of so-called "grain resistance" and "form resistance" [*Meyer-Peter and Müller*, 1948; *Parker and Peterson*, 1980; *Carson and Griffiths*, 1987; *Gomez and Church*, 1989; *Millar and Quick*, 1994; *Millar* 1999]. However, we think that these terms do not appropriately reflect the physical conditions in steep channels with shallow flows (see, for example, the discussion of *Rickenmann and Recking* [2011]). Therefore, the total flow resistance f_{tot} was considered to be composed of two main components: (1) the base-level resistance, f_0, which can be defined as the total resistance corresponding to deep flows, and (2) an additional resistance because of large roughness elements at a small relative flow depth, f_{add} [*Rickenmann and Recking*, 2011]. The latter refers to the same range of conditions as intermediate and large-scale roughness as defined by *Bathurst et al.* [1981]. In analogy to the grain/form flow resistance partitioning, the total flow resistance is the sum of the two components:

$$f_{tot} = f_0 + f_{add}. \quad (2)$$

[12] Such an additive approach has been applied previously, for example, by *Einstein and Banks* [1950], *Manga and Kirchner* [2000], *Ferguson* [2007], and *Comiti et al.* [2009].

[13] The studied flow resistance approaches used for bedload transport calculations are briefly described below.

If necessary, equations were modified from the original notation for better comparison. For further information, the reader is referred to the original publications. The flow resistance equations were combined with a bedload transport equation by using a reduced energy slope based on flow resistance partitioning [*Chiari et al.*, 2010] (see section 2.2).

2.1. Flow Resistance Equations

[14] *Whittaker et al.* [1988] presented design guidelines for river stabilization techniques with placed blocks in block ramps. The authors were interested in threshold conditions for the movement of blocks. In an experimental study they arranged blocks on a mobile bed in a flume and measured water and bed levels at equilibrium conditions for different tailwater levels. *Whittaker et al.* [1988] considered total shear stress acting on the flow as the sum of two components: resistance due to base material and to blocks. They calculated flow resistance due to base material f_0 after *Keulegan* [1938]:

$$\sqrt{\frac{8}{f_0}} = 2.5\ln\left(\frac{12r_h}{1.5D_{90}}\right), \tag{3}$$

where r_h is the hydraulic radius and D_x is the grain size for which x percent of the material is finer. Flow resistance due to the blocks (f_{add}) was expressed as

$$\sqrt{\frac{8}{f_{\mathrm{add}}}} = 2.5\ln\left(\frac{12r_h}{k_b}\right). \tag{4}$$

[15] Herein k_b is the roughness height associated with the blocks given as

$$k_b = \alpha D_b\left(17.8 - 0.47\frac{d}{D_b}\right), \tag{5}$$

in which D_b is the mean block diameter and α is the areal block concentration, given as

$$\alpha = N \cdot D_b^2, \tag{6}$$

where N is the number of blocks placed per square meter of bed. In equations (3) and (4), a logarithmic velocity profile is assumed, which is not true for flow around blocks in wake zones. But *Whittaker et al.* [1988] argued that at least with respect to velocity and water depth the trends given by a logarithmic law can be considered correct. They further assumed stationary and uniform flow and limited application of their approach to block concentrations $\alpha < 0.15$ and relative roughness in the range $0.5 < d/D_b < 4$.

[16] *Egashira and Ashida* [1991] developed a friction law for the flow over step-pool bed forms, taking into account the energy dissipation of the mean flow due to entrained eddies in separation zones and the energy dissipation in wall regions. They performed flume experiments for flows over artificial step-pool forms, finding a good agreement with their friction law. For flow resistance of the base material (f_0) along the sections between steps, they assumed a logarithmic law very similar to equation (3) to be valid:

$$\sqrt{\frac{8}{f_0}} = 2.5\ln\left(\frac{11r_h}{1.5D_{90}}\right). \tag{7}$$

[17] *Egashira and Ashida* [1991] found that both in sub- and supercritical flows, the rate of energy dissipation in the separation zone downstream from the crest plays an important role in the flow resistance. For the flow resistance in the region of the separation zone they gave

$$\sqrt{\frac{8}{f_{\mathrm{add}}}} = \sqrt{\frac{2r_h}{KE \cdot H}}, \tag{8}$$

in which KE is an empirical constant equal to 0.48, and H is the step height. The total flow resistance was given by

$$\sqrt{\frac{8}{f_{\mathrm{tot}}}} = \sqrt{\frac{8L}{aH(f_{\mathrm{add}} - f_0) + f_0 L}}, \tag{9}$$

where L is the step spacing and a is an empirical value, expressing the ratio between the length of the separation zone and the step height. The parameter a was suggested to take the value of 2.5, but might strongly vary for different stream conditions. Equations (8) and (9) suggest that flow resistance depends on the relative step height H/r_h, the step spacing L, and the resistance due to the base material f_0. In the case of chutes and pools the energy dissipation might also be controlled by hydraulic jumps, expressed in the term $\delta \cdot 8/(Fr^2 \cdot L)$, which needs to be added to the right-hand side of equation (9). δ is the energy loss due to hydraulic jumps and Fr is the Froude number. Fr and δ are difficult to determine for steep mountain rivers, and are therefore neglected in the calculations below.

[18] *Pagliara and Chiavaccini* [2006] conducted experiments in a steep laboratory flume to investigate flow resistance in the presence of boulders. The boulders were mimicked by metallic hemispheres with smooth and rough surfaces, arranged randomly or in rows over a granular base material. *Pagliara and Chiavaccini* [2006] found that the increase in flow resistance because of the boulders can be related to their areal concentration Γ, their disposition, and their surface roughness c. Two empirical equations were proposed to evaluate flow resistance, both in the presence (equation (10)) and the absence (equation (11)) of boulders:

$$\sqrt{\frac{8}{f_{\mathrm{tot}}}} = 3.5(1+\Gamma)^c S^{-0.17}\left(\frac{d}{D_{84}}\right)^{0.1}, \tag{10}$$

$$\sqrt{\frac{8}{f_0}} = 0.43\ln\left(S^{-2.5}\frac{d}{D_{84}}\right) + 2.8. \tag{11}$$

[19] The increase in flow resistance was found to be directly proportional to the boulder concentration Γ, where $\Gamma = n\pi D_B^2/(4WL)$, with n the number of boulders, W the width, and L the length of the reach. The exponent c in

equation (10) was empirically derived and depends on the disposition of the boulders (random or rows) and on the smoothness of the boulder surface (rounded or crushed). Rows of boulders act as sequences of steps, which produce intense flow accelerations and decelerations. Both equations (10) and (11) are recommended to be used for block ramps and constructed riprap channels in steep slopes (0.08–0.4) only, because they are characterized by a regular geometry that differs from natural mountain streams. Equation (10) is further limited to boulder concentrations of less than 0.3 [*Pagliara*, 2008].

[20] *Yager* [2006] studied the influence of immobile boulders on the stresses acting on mobile grains in steep, rough streams. She presented a theoretical flow resistance model that uses stress partitioning rather than empirical expressions to account for the resistance due to macroroughness. *Yager* [2006] hypothesized that the total bed shear stress can be partitioned into the shear stress borne by mobile grains and the stress borne by immobile grains with a characteristic diameter D_b. The total shear stress τ_t for a reach is given as the sum of the stress on immobile grains τ_I and the stress on the mobile grains τ_m, scaled with the area covered by the immobile (A_{IP}) and mobile grains (A_m), respectively, divided by the total bed area (A_t):

$$\tau_t = \frac{\tau_I A_{IP} + \tau_m A_m}{A_t}. \tag{12}$$

in which $\tau_m = \rho C_m v^2/2$, ρ is the density of water, and C_m is the drag coefficient for the mobile sediment. τ_I is given as $\tau_I = \rho A_{IF} C_I v^2/(2A_{IP})$, where A_{IF} is the bed perpendicular area of immobile grains, A_{IP} is the bed-parallel area occupied by the immobile grains, and C_I is the drag coefficient for immobile grains, calculated by $C_I = 157(d/p_u)^{-1.6}$, in which p_u is the portion of immobile grains that protrude above the mobile bed surface. Since immobile grains are often not isolated roughness elements, but arranged into clusters or steps, *Yager* [2006] assumed closely packed immobile grains in the cross-stream direction that have a characteristic downstream spacing λ_x. The total bed area is then given by $A_t = W\lambda_x$, the bed area occupied by immobile boulders is $A_{IP} = W\lambda_w$, where λ_w is defined here as the equivalent downstream length of the bed area occupied by boulders, and the area occupied by the mobile grains is $A_m = W\lambda_x - A_{IP}$. The cross-sectional area of the immobile grains A_{IF} (perpendicular to the flow) is a function of d, D_b and the upstream immobile grain protrusion p_u. *Yager* [2006] found the boulder density (which is given here by λ_w/λ_x) and the boulder protrusion to be main controls on shear stresses and flow velocities. Here we rewrite the shear stress of the mobile sediments τ_m and the shear stress of the immobile grains τ_I in terms of the Darcy-Weisbach friction factor, using the notation f_0 for the friction because of τ_m, and f_{add} for the friction due to τ_I:

$$\sqrt{\frac{8}{f_0}} = \sqrt{\frac{2}{C_m(1-\lambda_w/\lambda_x)}}, \tag{13}$$

$$\sqrt{\frac{8}{f_{\mathrm{add}}}} = \sqrt{\frac{2\lambda_x W}{A_{IF} C_I}}. \tag{14}$$

[21] Yager's theoretically based shear stress partitioning equations require little empirical calibration and may thus apply to a wide range of bed conditions. But they were tested only on a single set of simplified flume experiments [*Yager et al.*, 2007] and data of a single steep mountain stream [*Yager*, 2006].

[22] *Rickenmann and Recking* [2011] evaluated several flow resistance equations with 2890 individual field measurements of flow velocity in gravel bed rivers, including many steep streams. They concluded that the variable power flow resistance equation (VPE) of *Ferguson* [2007] gave the best overall performance. The VPE approach of Ferguson was used to develop a flow resistance partitioning approach for large- and intermediate-scale roughness conditions (in the sense of *Bathurst et al.* [1981]). A base-level resistance f_0 can be calculated with a Manning-Strickler type equation representing flow conditions with small-scale roughness:

$$\sqrt{\frac{8}{f_0}} = \frac{v_0}{\sqrt{g \cdot r_h \cdot S}} = 6.5\left(\frac{r_h}{D_{84}}\right)^{0.167} \tag{15}$$

in which, if used in the domains of large- and intermediate-scale roughness, v_0 is a virtual velocity characterizing flow conditions similar to those for which bedload transport equations were developed. For flow conditions with intermediate and large scale roughness, the total resistance f_{tot} can be calculated as

$$\sqrt{\frac{8}{f_{\mathrm{tot}}}} = \frac{v_{\mathrm{tot}}}{\sqrt{g \cdot r_h \cdot S}}, \tag{16}$$

in which v_{tot} is predicted with the VPE approach of *Ferguson* [2007]:

$$v_{\mathrm{tot}} = \frac{\sqrt{g \cdot r_h \cdot S} \cdot 6.5 \cdot 2.5\left(\frac{r_h}{D_{84}}\right)}{\sqrt{6.5^2 + 2.5^2\left(\frac{r_h}{D_{84}}\right)^{\frac{5}{3}}}}. \tag{17}$$

[23] The partitioning between base-level and total resistance is expressed as

$$\sqrt{\frac{f_0}{f_{\mathrm{tot}}}} = \frac{v_{\mathrm{tot}}}{v_0}. \tag{18}$$

[24] The approach represented by equations (15) to (18) is the only approach considered here that does not explicitly include a measure of large roughness elements in its equations. The proposed flow resistance partitioning is basically a function of relative flow depth. However, the information on mean roughness conditions is implicit in the data used to derive the equation. In earlier studies [*Badoux and Rickenmann*, 2008; *Chiari*, 2008; *Chiari et al.*, 2010; *Chiari and Rickenmann*, 2011; *Rickenmann*, 2005; *Rickenmann et al.*, 2006], a similar concept of flow resistance partitioning as proposed by equations (15)–(18) was applied to bedload transport calculations in steep streams. This earlier

flow resistance partitioning approach was based on 373 field measurements of flow resistance including shallow flows in steep streams [*Rickenmann*, 1994, 1996], in contrast to the 2890 field measurements used by *Rickenmann and Recking* [2011].

2.2. Bedload Transport Equations

[25] *Rickenmann* [1991] proposed a shear-stress-based equation to compute bedload transport. The equation is based on 252 laboratory experiments conducted by *Meyer-Peter and Müller* [1948], *Smart and Jäggi* [1983], and *Rickenmann* [1991] for a slope range of 0.0004 to 0.2, and can be written as

$$\Phi_b = \frac{3.1(D_{90}/D_{30})^{0.2}\sqrt{\theta}(\theta - \theta_c)Fr^{1.1}}{\sqrt{s-1}}. \qquad (19)$$

[26] Here the dimensionless bedload transport rate $\Phi_b = q_b/[(s-1)gD_{50}{}^3]^{0.5}$, q_b = bedload transport rate per unit of channel width, $s = \rho_s/\rho$ is the ratio of solid to fluid density, and the dimensionless shear stress $\theta = r_h\ S/[(s-1)D_{50}]$. The critical dimensionless shear stress at the initiation of bedload transport θ_c is determined here as

$$\theta_c = \frac{r_{hc} \cdot S}{(s-1)D_{50}}, \qquad (20)$$

where r_{hc} is the critical hydraulic radius corresponding to the critical discharge unit $q_{c,}$ which is calculated here with an empirical equation of *Bathurst et al.* [1987], slightly modified by *Rickenmann* [1991] (see Tables 1 and 2):

$$q_c = 0.065 \cdot (s-1)^{1.67}\sqrt{g}D_{50}^{1.5}S^{-1.12}. \qquad (21)$$

[27] For quartz particles in water with a relative density $s = 2.68$, *Rickenmann* [2001] simplified equation (19) to

$$\Phi_b = 2.5\sqrt{\theta}(\theta - \theta_c)Fr. \qquad (22)$$

[28] In the present study, equation (22) was used as a reference bedload transport equation that does not account for the effects of macro-roughness. For easier comparison with field data on bedload transport, equation (22) can be written as a function of unit discharge q [*Rickenmann*, 2001]

$$q_b = 1.5(q - q_c)S^{1.5}. \qquad (23)$$

[29] The bedload transport equation (22) was used in combination with the flow-resistance partitioning approaches described above to account for increased flow resistance. The combination procedure is on the basis of the earlier approaches of *Meyer-Peter and Müller* [1948], *Palt* [2001], and *Rickenmann* [2005], who introduced empirical functions to account for flow resistance because of macro-roughness through a reduced energy slope. With this method better agreement was obtained between observed and predicted bedload volumes for flood events in 2005 in Austrian and Swiss mountain streams [*Chiari*, 2008; *Chiari et al.*, 2010; *Chiari and Rickenmann*, 2011; *Rickenmann et al.*, 2006], and for several flood events in 2000 in Swiss mountain streams [*Badoux and Rickenmann*, 2008]. Using the Manning-Strickler or the Darcy-Weisbach equation, the total energy slope is given as

$$S = \frac{v^2 n_{\text{tot}}^2}{r_h{}^{4/3}} = \frac{v^2 f_{\text{tot}}}{8gd}. \qquad (24)$$

[30] The reduced energy slope associated with grain friction only, S_{red}, can be expressed as

$$S_{\text{red}} = \frac{v^2 n_0^2}{r_h{}^{4/3}} = \frac{v^2 f_0}{8gd}. \qquad (25)$$

[31] Thus, S_{red} can be determined with

$$S_{\text{red}} = S\left(\frac{n_0}{n_{\text{tot}}}\right)^e = S\left(\sqrt{\frac{f_0}{f_{\text{tot}}}}\right)^e. \qquad (26)$$

[32] *Meyer-Peter and Müller* [1948] showed theoretically that e may vary between 4/3 and 2, and from their flume experiments on bedload transport they empirically determined a best fit value of 1.5. For several bedload transporting flood events in 2005 in Switzerland and Austria, *Chiari and Rickenmann* [2011] found best fit values for e in the range of 1 to 1.5. We used a fixed value of $e = 1.5$ in our work. The flow resistance partitioning equations (section 2.1) were used to calculate S_{red}, which in turn was used to determine a reduced dimensionless shear stress $\theta_r = r_h\ S_{red}/[(s-1)D_{50}]$ instead of θ in the bedload transport equation (22):

$$\Phi_b = 2.5\sqrt{\theta_r}(\theta_r - \theta_{c,r})Fr. \qquad (27)$$

[33] Since equation (21) is an empirical equation, the reduced critical dimensionless shear stress $\theta_{c,r}$ was determined as

$$\theta_{c,r} = \frac{r_{hc} \cdot S_{\text{red}(r_{hc})}}{(s-1)D_{50}}, \qquad (28)$$

where both the critical hydraulic radius r_{hc} and the reduced energy slope at the critical hydraulic radius $S_{\text{red}(r_{hc})}$ were calculated for the critical discharge at initiation of bedload motion estimated with equation (21).

[34] The approach as outlined above needs the hydraulic radius as an input parameter for the calculations. Since only discharge information was available for the study streams, hydraulic parameters were back-calculated using field surveys of slope and channel cross sections (see section 3.2), assuming steady uniform flow using the flow resistance equation of *Smart and Jaeggi* [1983]. In a second step, resistance partitioning is applied through equation (26) to determine the part of the flow energy that is available for bedload transport.

[35] Alternative bedload transport calculations were performed with the modified equation of *Parker* [1990] in combination with the shear stress partitioning approach of *Yager* [2006]. This approach was added to the study to (1) show the influence of using a different transport model, and (2) because *Yager* [2006] found the best performance of

Table 1. Stream Characteristics, Description, and Sources of Discharge and Bedload Data for Streams With Long-Term Periodic Bedload Measurements ("Long-Term Data")

Stream Character	Erlenbach	Rotenbach	Schwändlibach	Rappengraben 1	Rappengraben 2	Sperbelgraben	Melera
Catchment area (km^2)	0.7	1.7	1.4	0.7	0.6	0.5	1.1
Elevation, lowest/highest (m)	1110/1655	1274/1630	1217/1642	983/1256	990/1256	911/1203	962/1773
Geology	Flysch	Flysch	Flysch	Conglomerate	Conglomerate	Conglomerate	Crystalline
Forest/glacier extent (%)	39/0	14/0	29/0	35/0	30/0	99/0	84/0
Channel type[a]	Step-pool	Step-pool	Step-pool	Plane bed	Plane bed	Plane bed	Step-pool
Discharge regime[b]	Nivo-pluvial prealpine	Nival	Nival	Pluvial supérieur	Pluvial supérieur	Pluvial supérieur	Nivo-pluvial
Mean annual precipitation[c] (mmol)	2300	1840	1840	1570	1570	1590	2060
Peak flow ($m^3 s^{-1}$)/return period[c] (years)	14.6[d]/50[d]	18/40–50	8.5/40–50	2.2/30–40	2.6/50–80	1.2/20–30	8/80–100
			Discharge Data Used				
Measurement	Stream gage[e]	Stream gage[f]	Stream gage[f]	Stream gage[e]	Stream gage[e]	Stream gage[e]	Stream gage[e]
Hydrograph time steps (min)	10	10	10	10	10	10	5
Critical discharge[g] ($m^3 s^{-1}$)	0.5	2.5	1.5	0.35	0.3	0.28	0.5
Peak flow of studied events ($m^3 s^{-1}$)	10.2	14.7	5.9	1.7	1.7	1.1	8
			Bedload Data Used				
Type of sediment measurement	Sediment retention basin[e]	Sediment retention basin[e]	Sediment retention basin[e]	Sediment trap[e]	Sediment trap[e]	Sediment trap[e]	Sediment retention basin[e]
Mean annual sediment yield (m^3)	603	138	69	58	77	42	162
Periods of sediment data used	1986–2010	1953–2010	1953–2010	1903–1927	1927–1957	1903–1953	1934–1951
Number of sediment surveys used	48	35	35	17	28	33	11
Fraction of bedload volume to total[h]	0.5	0.6	0.6	0.66	0.66	0.66	0.6

[a] After *Montgomery and Buffington* [1997].
[b] After *Weingartner and Aschwanden* [1992].
[c] *Rickenmann* [1997].
[d] *Turowski et al.* [2009].
[e] Operated by the Swiss Federal Research Institute WSL.
[f] Operated by the Swiss Federal Office for the Environment.
[g] Critical discharge for the initiation of bedload motion, estimated by *Rickenmann* [1997].
[h] Estimation, total sediment volume includes bedload, fines, and pores.

Table 2. Stream Characteristics, Description, and Sources of Discharge and Bedload Data, for Streams With Bedload Data of One Large Flood Event ("Event Data")

Stream Character	Lonza	Gamsa	Baltschieder	Saltina	Buoholzbach	Steinibach	Mattenbach
Catchment area (km^2)	170	38	43	78	13.9	12.2	30.8
Elevation, lowest/highest (m)	630/3994	660/3391	647/3934	670/3438	490/2404	493/1955	1015/2728
Geology	Gneiss	Gneiss	Gneiss, Granit	Gneiss	Flysch, Limestone	Flysch, Limestone	Flysch
Forest/glacier extent (%)	8/16	22/2	10/16	21/4	40/0	35/0	23/0
Channel type[a]	Cascade	Cascade	Step-pool	Plane bed	Step-pool	Step-pool	Cascade
Discharge regime[b]	Glacio-nival	Nivo-glaciaire	Glacio-nival	Glacio-nival	Nival-alpine	Nival-alpine	Nival-alpine
Mean annual precipitation[c] (mmol)	600–2400	1000–2400	600–2000	1000–2400	1200–2400	1200–2400	1400–2000
Discharge Data Used							
Type of discharge measurement	Runoff modeling[d]	Runoff modeling[e]	Runoff modeling[f]	Stream gage[g]	Rainfall-runoff-modeling[h]	Rainfall-runoffmodeling[h]	Rainfall-runoff modeling[h]
Hydrograph time steps (min)	30	30	30	30	5	5	5
Critical discharge[i] (m^3 s^{-1})	1.08	0.38	0.74	6.62	0.44	0.77	0.8
Peak flow (m^3 s^{-1})/return period (years)	90–95/100	65–70/-	~100/-	~120/80	~40/30–100[j]	~85/100–300[j]	~45/30[k]
Bedload Data Used							
Bedload volume estimation	Channel deposition depth[d]	Deposits[l]	Deposits[m]	Deposits[n]	Retention basin, deposits[j]	Retention basin, deposits[j]	Deposits[k]
Period of sediment data used	14–17 Oct 2000	14–15 Oct 2000	14–16 Oct 2000	13–19 Oct 2000	21–23 Aug 2005	21–23 Aug 2005	21–23 Aug 2005
Fraction of bedload volume to total[o]	0.66	0.66	0.66	0.66	0.66	0.66	0.66

[a]After *Montgomery and Buffington* [1997].
[b]After *Weingartner and Aschwanden* [1992].
[c]After *Kirchhofer and Sevruk* [1992].
[d]*Abgottspon et al.* [2001] and *BWG* [2002].
[e]Numerically modeled [*BWG*, 2002; *LCH-EPFL*, 2003].
[f]Peak flow from field vision, hydrograph from modified Clark model [*BWG*, 2002; *Jäggi et al.*, 2004].
[g]Operated by the Swiss Federal Office for the Environment.
[h]Authors work, model: HEC-HMS [*USACE*, 2000].
[i]Critical discharge for the initiation of bedload motion, calculated after *Bathurst et al.* [1987].
[j]*Oeko-B AG* [2006].
[k]*geo7* [1998].
[l]Photogrammetrically measured [*BWG*, 2002].
[m]*Jäggi et al.* [2004].
[n]*Burkhard and Jäggi* [2003].
[o]Estimation, total sediment volume includes bedload, fines, and pores.

this particular combination for the transport calculation for the Erlenbach, one of our study streams. The method of *Yager* [2006] further accounts for the limited availability of mobile sediment. The median grain size of the mobile fraction is used as a representative bedload size. In contrast to equation (22) it accounts for the effect of size-selective transport. The volumetric transport rate per unit width for each grain size class of the relatively mobile sediment q_{bmi} is

$$q_{\mathrm{bmi}} = \frac{(\tau_m/\rho)^{1.5} F_{mi} W^*_{mi}}{(\rho_s - \rho)/\rho}, \tag{29}$$

where F_{mi} is the volume fraction of the relatively mobile sediment that is in the ith grain size class, and W^*_{mi} is the dimensionless bedload transport rate of each grain size class. Instead of the total stress, *Yager* [2006] used the stress on the mobile sediment τ_m in equation (29). The total transport rate of all the grain sizes in the mobile sediment is given by

$$q_{Tm} = \left(\sum_{i=1}^{N} q_{\mathrm{bmi}}\right) \frac{A_m}{A_t}. \tag{30}$$

[36] The proportion of the bed area that is occupied by the mobile sediment (A_m/A_t) (compare equation (12)) is used to account for the limited availability of mobile sediment.

3. Study Streams and Field Data

3.1. Bedload and Discharge Data of Study Streams

[37] Data were collected from 13 mountain streams located in the Swiss Alps and Prealps (Figure 1, Tables 1 and 2), selected to cover a range of channel characteristics. For each of the streams some information on sediment transport was available. The streams feature alluvial channels with morphologies ranging from plane bed to cascade channel types and accentuated step-pool types [after *Montgomery and Buffington*, 1997], with channel slopes ranging from 2% to 19%. Two main groups of streams can be distinguished, one with periodic sediment yield measurements over several years or decades, and another with bedload data obtained after a single extreme transport event.

[38] The first group of streams (Table 1) includes six catchments with long series of measured sediment yield, here referred to as "long term data." In the Erlenbach catchment, deposited sediment volumes have been measured in a retention basin at least once each year since 1983 [*Hegg et al.*, 2006]. Since 1986, an indirect bedload sensor system has also recorded the impact of bedload grains transported over a measuring cross section right above the retention basin [*Bänziger and Burch*, 1990; *Rickenmann and McArdell*, 2007; *Turowski et al.*, 2009]. Bedload transport rates can be estimated from the sensor signal using a calibration relationship obtained from the measurements of deposited volumes in the retention basin [*Rickenmann and McArdell*, 2007]. For the streams Rappengraben, Sperbelgraben, Rotenbach, Schwändlibach, and Melera, discharge data was recorded by stream gaging stations [*Rickenmann*, 1997]. Sediment volumes delivered by these streams have been measured roughly once a year in sediment traps directly upstream of the gaging stations (Rappengraben and Sperbelgraben) or in sediment retention basins (Rotenbach, Schwändlibach, and Melera) [*Rickenmann*, 1997]. Thus, the bedload data integrate several transport events. More details about measurement facilities and sediment investigations can be found in the publication of *Zeller* [1985]; discharge and bedload data sets have been previously analyzed by *Rickenmann* [1997, 2001].

[39] The second group of study streams (Table 2) includes seven catchments, for each of which bedload data are available for a single exceptional transport event, here referred to as "event data." For four of the streams, the event was triggered by intense rainfall in the Canton Valais

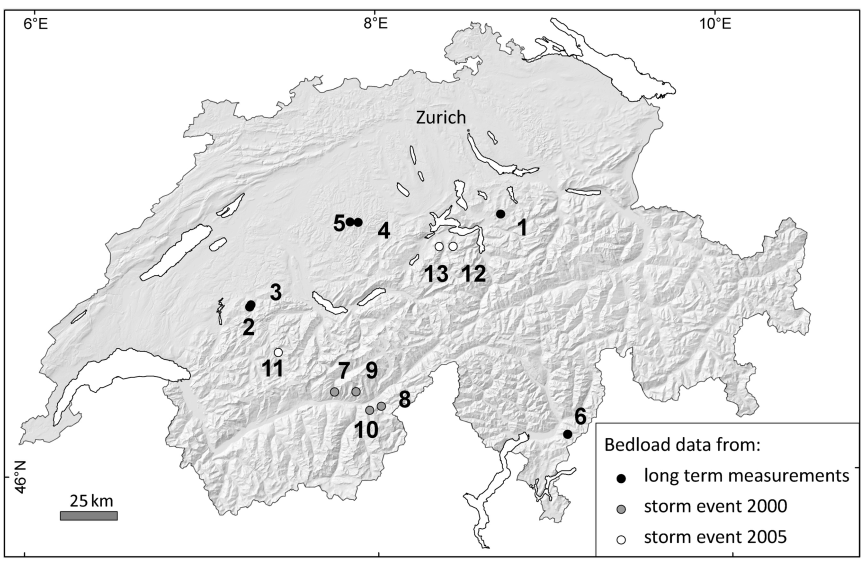

Figure 1. The locations of the study streams in Switzerland and types of bed load data; 1, Erlenbach; 2, Rotenbach; 3, Schwändlibach; 4, Sperbelgraben; 5, Rappengraben; 6, Melera; 7, Lonza; 8, Saltina; 9, Baltschieder; 10, Gamsa; 11, Mattenbach; 12, Buoholzbach; 13, Steinibach.

in the southwestern Swiss Alps in October 2000, one of the most severe flood events of the region in the twentieth century, causing 16 fatalities and total damage of around 710 million Swiss francs [*BWG*, 2002]. In several steep catchments, large amounts of sediment were transported and deposited on the alluvial fan at the confluence with the main valley river. Deposited sediment volumes were measured after well-documented events in the streams Lonza, Saltina, Baltschieder, and Gamsa, and are used in this study. Bedload data from these streams were previously described and compared to simple transport equations by *Badoux and Rickenmann* [2008]. The hydrographs for the Saltina and Lonza streams were measured at a stream gaging station, while the hydrographs for the Baltschieder and Gamsa were reconstructed from flood marks and rainfall-runoff modeling. For the other three streams the sediment transport events were triggered by intense precipitation in the northern part of the central Alps in August 2005, when 220 mm of rain fell within 72 h, causing six fatalities and total damage of three billion Swiss francs [*Bezzola and Hegg*, 2007, 2008]. This precipitation event was estimated to have a recurrence interval of over 100 years at 22 rain gaging stations of MeteoSwiss (MeteoSwiss 2006), and led to large changes in stream morphology and sustained fluvial sediment transport in 39 mountain streams. Here we use bedload data for the streams Buoholzbach, Steinibach, and Mattenbach, where transport estimates were based on the deposited sediment volumes in sediment retention basins, and on the number of truck loads used for sediment removal from overbank deposits outside of the retention basins [*Bezzola and Hegg*, 2007; *Rickenmann and Koschni*, 2010]. Direct discharge measurements were not available and the hydrograph was estimated using HEC-HMS [*U. S. Army Corps of Engineers*, 2000], a deterministic rainfall-runoff-routing model. Simulations were calibrated using peak flow estimates based on flood marks in the channel. Because of a lack of validation data we neglected uncertainty in discharge, which, however, would affect each transport prediction method in the same way and may not alter the general pattern of the results.

[40] The uncertainty of the measured sediment volumes is variable. For the first group, where the sediments were measured in retention basins and traps, we estimated from repeat measurements an uncertainty of less than 5% in volume. For the second stream group, we relied on measurements of engineers and local authorities shortly after the flood events. On the basis of their detailed reports, the volumes are likely to have an uncertainty of less than 25%. However, we corrected bulk sediment volumes for pore space and fine material that was not transported as bedload. For the large flood event data and the Rappengraben and Sperbelgraben, where sediments were measured in small sediment traps, we assumed that because of the turbulent flow there was no significant deposition of suspended load. For these streams, pore volume was estimated to be one-third of the total volume (Tables 1 and 2). For the Erlenbach we followed the observations of *Rickenmann* [1997], who estimated that about half of the bulk sediment volume in the large retention basin consisted of bedload material (Table 1). For the Rotenbach, Schwändlibach, and Melera suspended material was assumed to have been partially deposited in the somewhat smaller retention basins, implying a likely correction factor between two-thirds and one-half. We therefore used an intermediate value of 0.6 (Table 1).

3.2. Field Measurements of Channel Characteristics

[41] Channel roughness parameters necessary to evaluate the tested flow resistance and transport equations were measured in the 13 study streams (Table 3). Several approaches are sensitive to a measure of immobile boulders. We used a critical size of 0.5 m to define boulders throughout the study. The choice of this value is further discussed in section 5.3. Some field values, e.g., step spacing or width, vary considerably in a given reach. Here, reach-averaged values were used because calculations were made at the reach scale. Measurements were made for the reach with the lowest bedload transport capacity, because the behavior of this reach limits transported bedload volumes for all sections further downstream. Assuming that channel bed slope is the parameter limiting transport capacity, the surveys have been carried out in the reaches of the stream with the lowest bed slope, which coincides with the study streams with the reaches just upstream of the deposition areas. The reach length varied for the 13 streams, ranging from 10 to 34 times the bankfull-stream width; these reach lengths are adequate for relating stream morphology to channel processes [*Montgomery and Buffington*, 1997]. For the hydraulic calculations we used an irregular channel profile for each stream, obtained by averaging at least 10 manually measured cross sections in each study reach. See Table 3 for additional parameter definitions.

4. Results and Interpretation

4.1. Flow Resistance Calculations

[42] The roughness measures used in the flow resistance equations varied greatly between the streams. The characteristic grain sizes showed a tendency to increase with channel slope (Figure 2a). There is no such tendency between Γ and step slope *H/L*, which is the aspect ratio of step height *H* and step length *L*. This suggests that steps and boulders can be independent roughness features (Figure 2b).

[43] Flow resistance partitioning in terms of $(f_0/f_{tot})^{0.5}$ varied considerably across the different approaches over a large range of relative flow depths in the domain of large- and intermediate-scale roughness. For a given relative flow depth the values for $(f_0/f_{tot})^{0.5}$ calculated with a single approach can span almost the complete possible range from 0 to 1 (Figure 3). Large differences in $(f_0/f_{tot})^{0.5}$ arose even if the approaches were on the basis of similar measures of roughness. For example, both *Whittaker et al.* [1988] and *Pagliara and Chiavaccini* [2006] use boulder concentration as a roughness measure, but the former approach predicted low $(f_0/f_{tot})^{0.5}$ values around 0.2, while the latter approach predicted almost constantly high values around 0.8 (Figure 3) for transport-relevant flows. This might reflect the different concepts and experimental conditions under which the approaches have been developed.

[44] The four examples in Figure 3 show calculations for streams with different densities and distributions of macro-roughness. The Saltina (Figure 3a) features the lowest slope of the study streams, with intermediate values for boulder concentration and step spacing. At the Sperbelgraben

Table 3. Measured Reach Parameters

Parameter	Symbol	Rotenbach	Rappengraben 1	Schwändlibach	Sperbelgraben	Rappengraben 2	Erlenbach	Melera	Saltina	Lonza	Baltschieder	Mattenbach	Gamsa	Buoholzbach	Steinibach
Channel slope[a]	S	0.051	0.06	0.098	0.101	0.106	0.115	0.17	0.02	0.064	0.135	0.15	0.165	0.17	0.186
D_{30}[b] (m)	D_{30}	0.02	0.01	0.02	0.02	0.01	0.03	0.02	0.02	0.02	0.03	0.03	0.02	0.03	0.04
D_{50}[b] (m)	D_{50}	0.05	0.03	0.03	0.04	0.03	0.07	0.04	0.06	0.05	0.07	0.07	0.05	0.07	0.12
D_{84}[b] (m)	D_{84}	0.18	0.08	0.16	0.08	0.08	0.29	0.16	0.16	0.20	0.18	0.45	0.14	0.23	0.92
D_{90}[b] (m)	D_{90}	0.25	0.10	0.21	0.09	0.10	0.39	0.22	0.19	0.30	0.21	0.72	0.16	0.54	1.24
Bankfull width[c] (m)	W	5.63	4.98	4.96	5.43	4.98	4.70	5.57	14.14	12.44	11.68	13.50	11.80	9.76	8.00
Bottom width[c] (m)	W_{base}	3.75	4.20	3.50	3.00	3.50	3.50	4.00	12.00	9.50	9.00	11.00	9.50	7.00	6.00
Boulder concentration[d]	Γ	0.02	0	0.04	0	0	0.11	0.02	0.08	0.09	0.16	0.26	0.16	0.10	0.40
Mean boulder diameter[e] (m)	D_b	0.63	-	0.75	-	-	0.82[f]	0.72	1.03	1.00	1.31	1.02	1.16	1.07	1.06
Mean step length[g] (m)	L	10.45	22.91	16.19	60.83	22.91	7.86	15.32	31.39	17.78	7.84	10.85	16.48	10.00	50.83
Mean step height[g] (m)	H	0.51	1.58	0.81	1.00	1.58	0.69	1.04	1.65	1.04	1.13	0.98	3.02	2.12	2.73
Step slope[g]	H/L	0.049	0.069	0.050	0.016	0.069	0.088	0.068	0.053	0.058	0.144	0.09	0.183	0.212	0.054
Immobile grain step spacing[h] (m)	λ_x	29.64	-	13.24	-	-	4.00	26.38	10.12	9.17	6.40	3.12	5.57	8.30	2.07
Downstream length of immobile-grain steps[h] (m)	λ_w	0.63	-	0.75	-	-	1.30	0.72	1.03	1.00	1.31	1.02	1.16	1.07	1.06
Height of sediment above base of imm. grains[i] (m)	z_m	0.25	-	0.32	-	-	0.31	0.38	0.40	0.39	0.55	0.63	0.56	0.47	0.47
Immobile grain protrusion[i] (m)	p_u	0.38	-	0.43	-	-	0.13	0.34	0.63	0.61	0.77	0.39	0.60	0.60	0.60
Drag coefficient for the mobile sediment[h]	C_m	0.44	0.44	0.44	0.44	0.44	0.44	0.44	0.44	0.44	0.44	0.44	0.44	0.44	0.44
Median grain size of mobile sediment[j] (m)	D_{50m}	0.05	0.03	0.03	0.04	0.03	0.06	0.04	0.06	0.05	0.07	0.07	0.05	0.07	0.10
Coefficient boulder surface[k]	c	−2.40	−2.40	−2.40	−2.40	−2.40	−2.40	−2.40	−2.40	−2.40	−2.40	−2.40	−2.40	−2.40	−2.40
Block concentration[l]	α	0.02	0	0.06	0	0	0.14	0.03	0.10	0.11	0.20	0.32	0.20	0.13	0.50

[a]Mean channel slope of the study reach.
[b]Grain sizes were calculated after *Fehr* [1987] on the basis of line-by-number pebble counts of around 500 grains down to 1 cm in diameter for each study reach.
[c]Average of field measurements which were taken at least every 10 m.
[d]After *Pagliara and Chiavaccini* [2006].
[e]Considered are grains with *b*-axis diameter larger than 0.5 m.
[f]*Yager et al.* [2007] gives a value of 0.44.
[g]Derived from longitudinal profiles by laser slope and distance meter, where H is the vertical distance between the top of the step to the bottom of the pool and L is the effective distance between step tops; a step was identified if the step height exceeded 0.5 m and a pool existed (i.e., negative or very flat positive gradients).
[h]After *Yager* [2006].
[i]After *Yager* [2006] with $z_m = D_b - p_u$, in which p_u is the portion of an immobile grain that protrudes above the mobile bed surface that is upstream of the steps.
[j]Derived from the grain size distribution excluding grains larger than D_b.
[k]Coefficient describing boulder disposition and boulder surface texture after *Pagliara and Chiavaccini* [2006].
[l]After *Whittaker et al.* [1988].

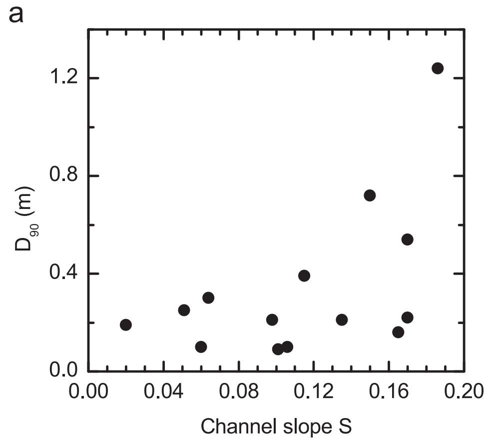

Figure 2. The relationship between measured roughness parameters. Each point represents one study stream.

(Figure 3b), sediment grains are relatively small and boulders are absent, but the channel bed is stepped, forced by the underlying bedrock. The Erlenbach (Figure 3c) has an intermediate boulder concentration, step slope, and bed slope, and the Gamsa stream (Figure 3d) is characterized by a high boulder concentration and a steep step and bed slope. For the comparatively rough Gamsa stream, the approaches of *Egashira and Ashida* [1991], *Whittaker et al.* [1988], and *Yager* [2006] all resulted in a relatively small fraction of grain resistance f_0 for all flow conditions. The same approaches gave higher $(f_0/f_{tot})^{0.5}$ values for the Erlenbach, because it features less macro-roughness elements. For the Sperbelgraben the same approaches resulted in a f_0 fraction of 1. There, only the approach of *Egashira and Ashida* [1991], which exclusively accounts for step-pool geometry, yielded a significant portion of additional roughness f_{add}, while the approach of *Rickenmann and Recking* [2011] resulted in decreasing $(f_0/f_{tot})^{0.5}$ values with decreasing r_h/D_{84} for all streams.

[45] Considering all 14 of the studied stream reaches, the approaches of *Rickenmann and Recking* [2011] and, above a threshold value of r_h/D_{84} of about 1–2, also those of *Yager* [2006] and *Whittaker et al.* [1988], always showed an increase in the fraction of base-level resistance f_0 with

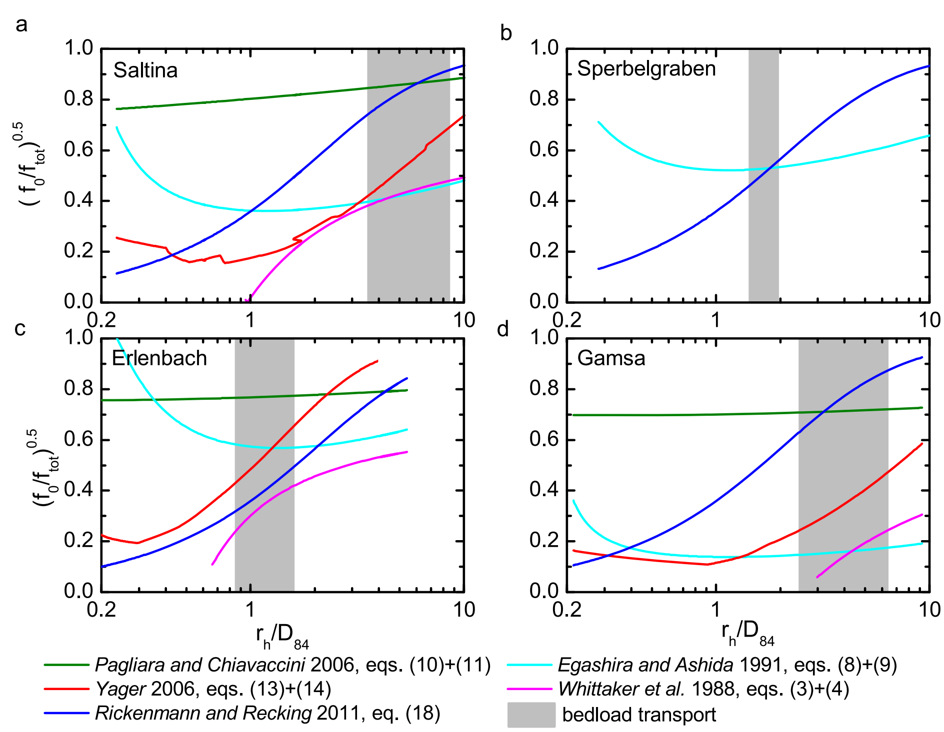

Figure 3. Fraction of base-level resistance to total resistance in terms of $(f_0/f_{tot})^{0.5}$ for a range of relative flow depths (r_h/D_{84}). The colored lines give the predictions by the respective approach (see Table 4). Gray areas indicate the range of relative flow depths, defined by the flow conditions for which 90% of the bedload transport occurred during the studied transport events.

Table 4. Tested Combinations of Bedload Transport and Flow Resistance Equations With Abbreviations

Bedload Transport	Equation	Flow Resistance Partitioning	Equation	Abbreviation
Rickenmann [2001]	equation (22)	no reduction	-	Ri-no
Rickenmann [2001]	equation (27)	*Pagliara and Chiavaccini* [2006]	equation (10) + (11)	Ri-PC
Rickenmann [2001]	equation (27)	*Whittaker* et al. [1988]	equation (3) + (4)	Ri-W
Rickenmann [2001]	equation (27)	*Egashira and Ashida* [1991]	equation (8) + (9)	Ri-EA
Rickenmann [2001]	equation (27)	*Yager* [2007]	equation (13) + (14)	Ri-Y
Rickenmann [2001]	equation (27)	*Rickenmann and Recking* [2011]	equation (18)	Ri-RR
Parker [1990]	equation (30)	*Yager* [2007]	equation (13) + (14)	P-Y

increasing relative flow depth, and the three methods yielded partly similar trends and $(f_0/f_{tot})^{0.5}$ values. The approaches of *Egashira and Ashida* [1991] and *Pagliara and Chiavaccini* [2006] were less sensitive to relative flow depth, and the fraction of $(f_0/f_{tot})^{0.5}$ varied only slightly within the considered range of relative flow depths. The approach of *Pagliara and Chiavaccini* [2006] yielded for each stream an almost constant value of $(f_0/f_{tot})^{0.5}$.

4.2. Bedload Volume Calculations

[46] In this section bedload transport calculations are presented, computed with the equation of *Rickenmann* [2001] and a modified *Parker* [1990] equation. The Rickenmann equation (equation (27)) was combined with all flow resistance partitioning approaches as described in section 2.2. The Parker equation was used in a form modified by *Yager* [2006] (equation (30)) to account for the stresses acting on the mobile sediment only. The combinations of equations and their abbreviations used below are listed in Table 4. The combinations are evaluated by the discrepancy ratio V_{pred}/V_{meas}, which is the ratio of predicted to measured bedload volumes.

[47] The equations' performance was highly variable for different streams and individual transport events. In Figure 4 the distributions of V_{pred}/V_{meas} values for individual events are shown for each stream. Many approaches showed a large variation of V_{pred}/V_{meas} spanning one to three orders of magnitude. This can be attributed to the large range of flow conditions observed for the streams and the sensitivity of the approaches to these. The reference equation of *Rickenmann* [2001] (Ri-no) with no accounting for macro-roughness overpredicted transport volumes by up to two orders of magnitude. Compared to this reference, for streams that feature macro-roughness, all other combinations of equations predicted smaller transport volumes through stress partitioning. The prediction of bedload volumes for large flood events (Figure 4, scatter plots) is generally better than for the long-term bedload data (Figure 4, box plots), which also included small transport events with smaller relevant r_h/D_{84} ratios than the long-term data (see Figure 3).

[48] To study the sensitivity of these approaches to several stream characteristics, the streams were grouped according to (1) high and low boulder concentration, (2) large and small step slope, and (3) event magnitude (Table 5). In this way, it is possible to characterize the conditions under which an approach might be more or less suitable. The boulder-based approaches (Rickenmann-Pagliara and Chiavaccini [Ri-PC], Rickenmann-Whittaker [Ri-W], and Rickenmann-Yager [Ri-Y]; see also Table 4) gave better bedload volume predictions for streams with high boulder concentrations and large step slopes (Figure 5), compared to streams with less pronounced macro-roughness. Furthermore, the predictions were better for approaches with a stronger physical component, i.e., Ri-Y and Ri-W performed somewhat better than Ri-PC. For streams with low boulder concentrations or small step slopes, the variability in bedload prediction was high, spanning more than an order of magnitude (Figure 5). The approach of *Yager* [2006], both in combination with the transport equations of *Rickenmann* [2001] (Ri-Y) and *Parker* [1990] (P-Y), gave median V_{pred}/V_{meas} values within an order of magnitude around the observed bedload volumes for streams with high boulder concentration. However, the combination Ri-Y consistently worked better than P-Y, which gave the largest median overprediction of bedload volumes for the complete data set. This indicates that the bedload transport equation of *Rickenmann* [2001] (equation (22)) may be more suitable for the studied streams than that of *Parker* [1990] (equation (30)). Moreover, the modified Parker equation (P-Y) was extremely sensitive to the magnitude of the flood event. The approach of *Egashira and Ashida* [1991] (Ri-EA), which explicitly considers the step slope *H/L*, yielded V_{pred}/V_{meas} ratios that varied over 1.5 orders of magnitude, which is the largest variation observed among all of the tested equations. The median V_{pred}/V_{meas} ratio indicated systematic underprediction of measured bedload volumes, except for the streams with small step slope. Thus, the correction of the energy slope appears to be too large in the approach of *Egashira and Ashida* [1991]. The combination Ri-RR generated relatively unbiased median V_{pred}/V_{meas} values between 0.8 and 1.6 for all stream groups with a relatively small variability within each group (Figure 5).

[49] For streams with high boulder concentration Γ, the combinations Ri-Y, P-Y, Ri-PC, Ri-W, and Ri-RR yielded median V_{pred}/V_{meas} values close to 1 (Figure 6). Except for the approach of Rickenmann and Recking (Ri-RR), all of these approaches calculated flow resistance on the basis of boulder concentration. Bedload transport in streams with distinct step-pool structure was best predicted by the combinations Ri-RR, Ri-W, Ri-Y, and Ri-PC.

[50] In Figure 7 the performance of the combinations is shown related to three data groups, of which one contains data from streams with long-term periodic bedload observations and a wide distribution of flood sizes ("long-term data"). A second group includes the data of streams with a single large flood ("event data"). The third group ("all data") consists of the event data and the sums of the long-term data. The best predictions for the long-term data were attained by Ri-W, Ri-RR, and Ri-Y, which predicted 71%, 64%, and 63% of the events to within a factor of 3 of the observed bedload volumes, respectively (Figure 7). The V_{pred}/V_{meas} values for all combinations of equations ranged

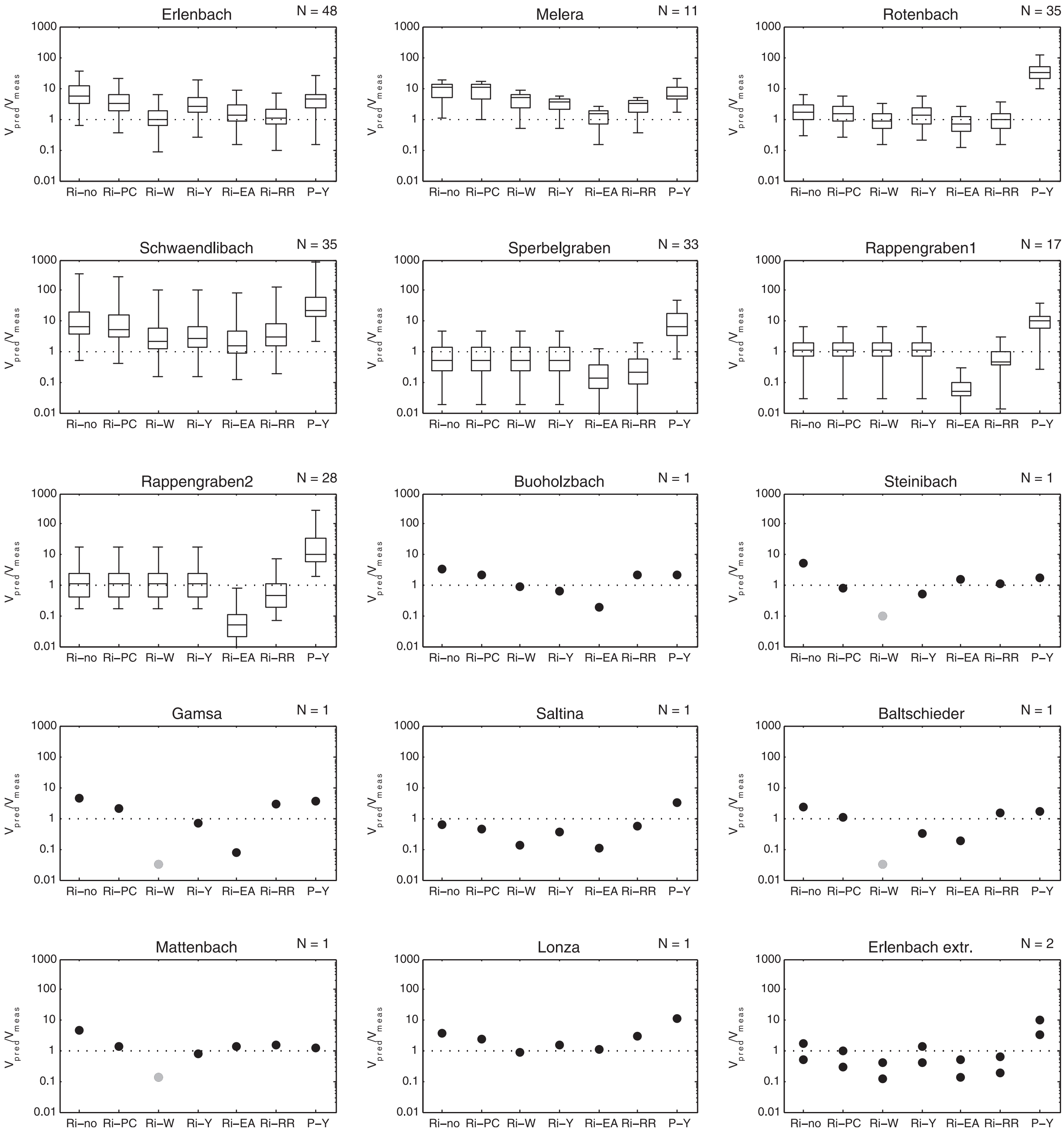

Figure 4. Ratios of predicted to measured bedload volumes (V_{pred}/V_{meas}) for each study stream, calculated with the bedload equation of *Rickenmann* [2001] in combination with flow-resistance partitioning approaches and the modified Parker bedload equation [*Parker*, 1990] by *Yager* [2006] (defined in Table 4). The light gray color indicates that a given approach is not applicable. N is the number of considered transport events per stream. The dashed lines indicate the values for perfect agreement of predictions and measurements. The boxes define 25th- and 75th-percentile and median. Whiskers are 5th- and 95th-percentile of the data. The plot "Erlenbach extr." additionally contains separate data of the two largest floods of the Erlenbach.

from 0.04 to 59 (10th and 90th percentile). The combinations Ri-W and Ri-RR gave the best median V_{pred}/V_{meas} value for the long-term data, which suggests a good overall performance (Figure 7, Table 6). However, the coefficient of variation for both combinations is comparable to that for most other tested combinations. The smallest coefficient of variation was exhibited by the combination Ri-Y (Table 6). For the large flood event data, the combination Ri-Y was the only approach in which all predictions fell within a factor of 3 of the observed volumes. However, the combination

Table 5. Definition of Data Groups[a]

Group Name	Definition	Streams Included
Γ-high	Boulder concentration $\Gamma \geq 0.1$	Gamsa, Baltschieder, Buoholzbach, Steinibach, Mattenbach, Erlenbach
Γ-low	Boulder concentration $\Gamma \leq 0.1$	Melera, Rotenbach, Schwändlibach, Sperbelgraben, Rappengraben1 + 2, Saltina, Lonza
H/L-large	Step slope $H/L > 0.068$	Gamsa, Baltschieder, Buoholzbach, Mattenbach, Erlenbach, Rappengraben1 + 2
H/L-small	Step slope $H/L \leq 0.068$	Melera, Rotenbach, Schwändlibach, Sperbelgraben, Steinibach, Saltina, Lonza
Event data	Data of large flood events only	Buoholzbach, Steinibach, Gamsa, Saltina, Baltschieder, Mattenbach, Lonza, Erlenb._extr.
Long term data	Data of long-term bedload series	Erlenbach, Melera, Rotenbach, Schwändlibach, Sperbelgraben, Rappengraben1 + 2
All data	Entire data set	Event data + long term data (sums of each stream)

[a]For the streams Gamsa, Baltschieder, Steinibach, and Mattenbach the predictions with the approach Rickenmann-Whittaker (Ri-W) were excluded, because these streams were out of the application range.

Ri-PC gave the best median agreement with the measurements for large flood events. The combination Ri-EA gave the lowest median V_{pred}/V_{meas} value, underpredicting more than 70% of the bedload transport events. The best median prediction for the complete data set including all studied streams was given by the empirical approach Ri-RR with $V_{pred}/V_{meas} = 1.0$ and 88% of the events were predicted within a factor of 3 of the observed volumes. The median values of the boulder approaches Ri-Y and R-W were only marginally worse. Ri-Y predicted 93% of the events within a factor of 3 of the observed.

5. Discussion

[51] The analyses presented above show that predictions of bedload volumes are significantly improved by taking into account macro-roughness using flow resistance partitioning. The partitioning was used to account for additional energy "losses" due to macro-roughness elements or increased total flow resistance in steep streams with shallow flows. Predicted bedload volumes differed among the tested approaches, primarily because of the choice of the transport formula and secondarily because of the resistance partitioning approach.

5.1. Choice of Bedload Transport Equation

[52] Our approach of reducing the energy slope in the bedload transport equations may have different effects on different bedload transport equations. However, the relative differences in the resulting bedload volumes V_{pred} are small. This is because most of the bedload equations that are applicable to steep streams are dependent on excess shear stress in a similar manner. The dominant differences lie in the calculation of the critical shear stress, which in turn affects only predictions near the initiation of the bedload transport. Our data, however, are dominated by flows with elevated discharges, i.e., we have high excess shear stresses, for which many bedload equations give similar relationships [e.g., *Gomez and Church*, 1989]. Moreover, it has been shown by *Recking et al.* [2008] in a comparison with more than 1000 experimental observations that our reference equation of *Rickenmann* [2001] yielded similar

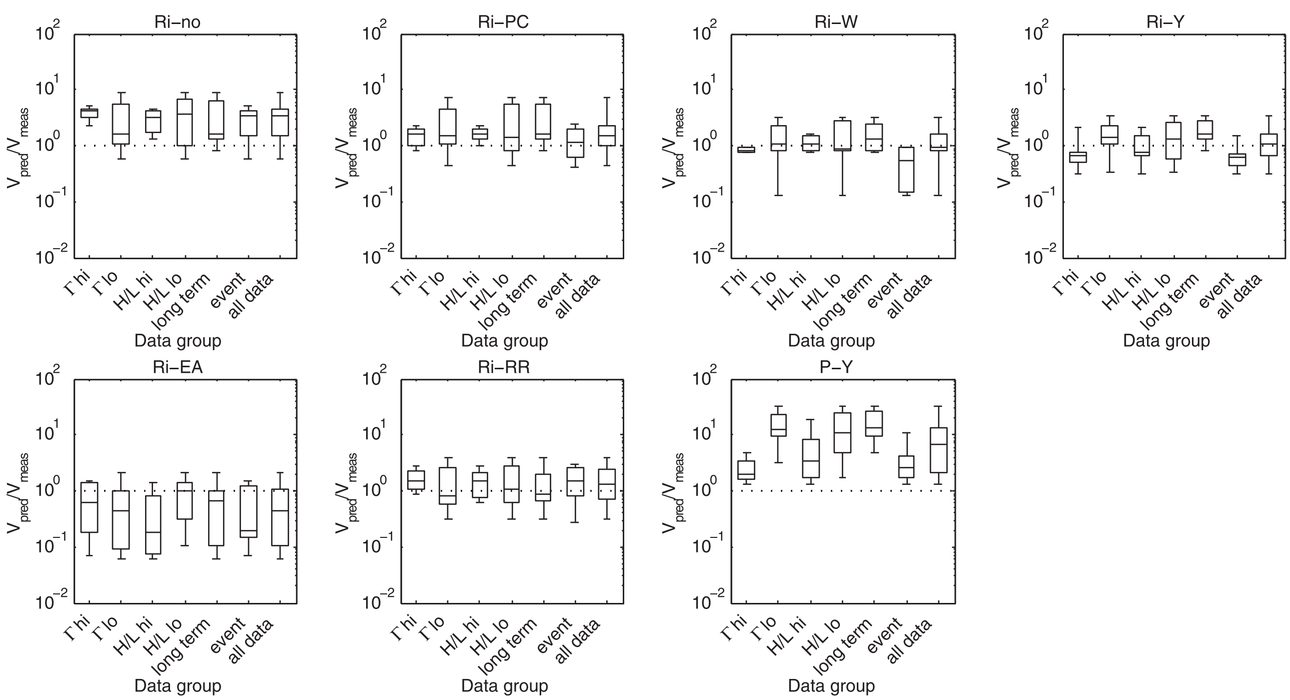

Figure 5. The ratios of predicted to measured bedload volumes (V_{pred}/V_{meas}). Each plot illustrates the performance of one equation combination (Table 4). The dashed lines indicate the values for perfect agreement of predictions and measurements. The data set is grouped according to Table 5.

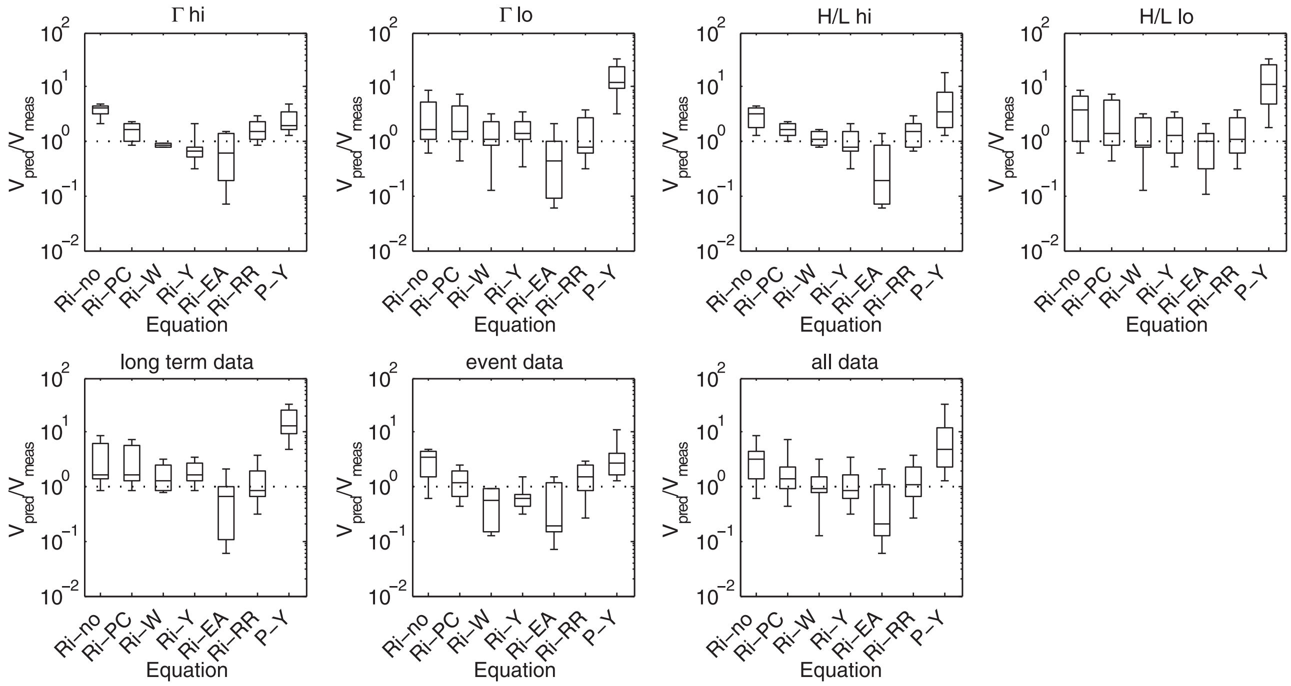

Figure 6. The ratios of predicted to measured bedload volumes (V_{pred}/V_{meas}). Each plot gives the performance of the tested equations (Table 4) for a stream type group according to Table 5. The dashed lines indicate perfect agreement between predictions and measurements.

deviations from measured bedload rates than other excess shear stress equations (e.g., those of *Schoklitsch* [1962], *Julien* [2002], *Abrahams and Gao* [2006]). Consequently, using different bedload equations will have only small effects on the resulting order of the reduction. Thus, the pattern for the predicted bedload volumes V_{pred} would be similar regardless of the applied bedload transport equation. Since we wanted to focus on the resistance partitioning approaches and we did not want to introduce another source of variability, we limited the number of bedload equations in the present study. We mainly used the equation of *Rickenmann* [2001] because it was developed for steep slope conditions as in our study streams. One alternative bedload equation was tested in combination with the flow resistance approach of *Yager* [2006], namely the equation of *Parker* [1990], because it has shown the best predictive performance in the study of *Yager* [2006]. A comprehensive test of different bedload transport equations is beyond the scope of this paper.

5.2. Performance of Flow Resistance Approaches

[53] Most of the tested approaches to flow resistance partitioning have an empirical component, and the results indicate that a specific approach may not apply to a range of streambed and flow conditions much wider than the range of conditions from which the approach was developed. Most equations performed better for large flow events, for which the relative flow depth was large, the excess shear stress was very high, and the majority of all sediment sizes may have been mobile; this finding is in agreement with other studies [e.g., *Bathurst et al.*, 1987; *D'Agostino and Lenzi*, 1999; *Rickenmann*, 2001]. The data from the large flow events were associated with a higher proportion of transport duration with large relative flow depths than the long-term data series.

[54] Compared to the reference equation by *Rickenmann* [2001] (Ri-no), which does not account for macro-roughness, the boulder approach of *Pagliara and Chiavaccini* [2006] in combination Ri-PC consistently reduced transport rates for streams with substantial concentrations of large boulders and streams with large step slopes. However, the nearly constant value of $(f_0/f_{tot})^{0.5}$ predicted by the flow resistance equation of *Pagliara and Chiavaccini* [2006] for changing relative flow depth is implausible and not supported by the other tested flow resistance approaches. Nevertheless, at relative flow depths that are relevant for bedload transport, the approach predicted similar $(f_0/f_{tot})^{0.5}$ values as the empirical approach of *Rickenmann and Recking* [2011]. The concordance may be coincidental, because for smaller flow depths, $(f_0/f_{tot})^{0.5}$ values for the approach of *Pagliara and Chiavaccini* [2006] were very high relative to predictions by the empirically broadly supported equation by *Rickenmann and Recking* [2011] and relative to the physically based equation of *Yager* [2006]. The validity of the *Pagliara and Chiavaccini* [2006] approach is thus questionable, particularly for smaller relative flow depths. However, although *Pagliara* [2008] restricted the flow resistance calculation used in combination Ri-PC to channel slopes in the range of 0.08 to 0.4 and boulder concentrations smaller than 0.3, the calculated V_{pred}/V_{meas} values are of similar order outside this range as inside.

[55] The approach of *Whittaker et al.* [1988], combination Ri-W, was very sensitive to boulder concentration and relative flow depth, which resulted in highly variable values of $(f_0/f_{tot})^{0.5}$. The approach is limited to block concentrations smaller than 0.15 [*Whittaker et al.*, 1988]. In fact,

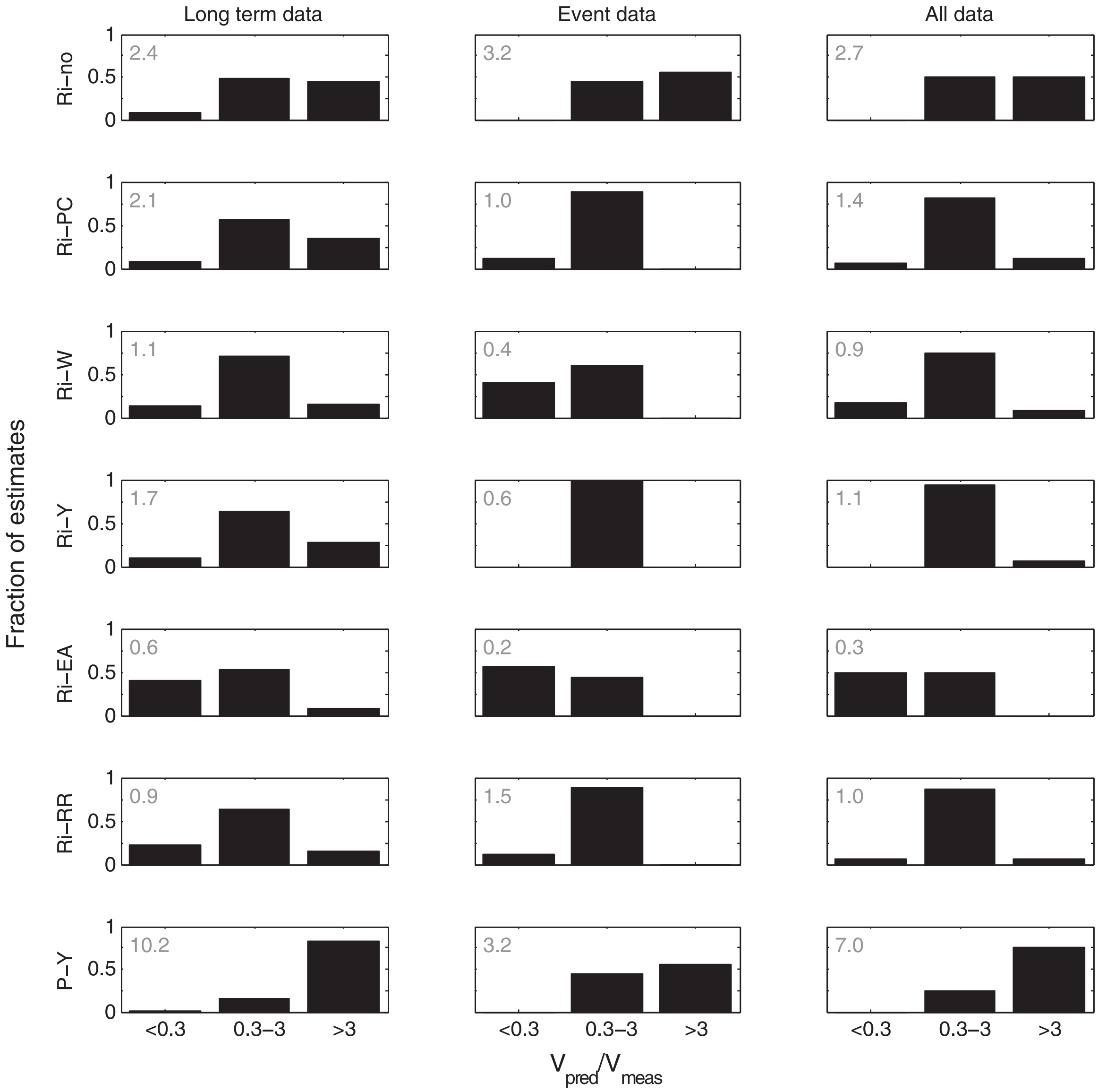

Figure 7. The ratios of predicted to measured bedload volumes ($V_{\mathrm{pred}}/V_{\mathrm{meas}}$) calculated with the partitioning approaches (defined in Table 4) separated into three data groups (defined in Table 5). $V_{\mathrm{pred}}/V_{\mathrm{meas}}$ ratios are given in three classes, of which the central class represents values within a factor of 3 around $V_{\mathrm{pred}}/V_{\mathrm{meas}} = 1$, which represents good agreement between prediction and measurement. The numbers in gray give the median $V_{\mathrm{pred}}/V_{\mathrm{meas}}$ ratio for the corresponding approach and data group. The data group "long-term data" includes 207 bedload transport events (see Table 1), the data set "event data" includes nine extreme events (see Table 2). The combined set "all data" includes the bedload sums of each study stream, to give equal weight to the calculations in each stream, regardless of the number of studied events. The approach of *Whittaker et al.* [1988] (Ri-W) was not applied to four of the study streams, thus "event data" and "all data" include only 5 and 12 data points, respectively.

predicted flow resistance was only plausible for streams with small boulder concentrations. Four of our study streams have larger block concentrations (Baltschieder, Mattenbach, Gamsa, and Steinibach). For these streams the flow resistance due to boulders is overestimated and the transported bedload volumes were underestimated by an order of magnitude. Consequently, these calculations were excluded from the analysis (compare Figure 4, gray dots). The good performance in streams with high boulder concentrations and large step slopes was thus based on the data of only two and six streams, respectively.

[56] The approach by *Egashira and Ashida* [1991], combination Ri-EA, was highly sensitive to the step slope H/L. The small predicted values of $(f_0/f_{\mathrm{tot}})^{0.5}$, because of steps and pools, led to a significant increase in total flow resistance. As a result, Ri-EA underpredicted the measured bedload volumes. Compared to the other combinations, Ri-EA gave the smallest median $V_{\mathrm{pred}}/V_{\mathrm{meas}}$ value for the complete

Table 6. Scores for Predicted/Measured Bedload Volumes (V_{pred}/V_{meas}) for Each Equation Combination and Data Set[a]

	Long-Term Data					Event Data					All Data				
	P_{10}	P_{90}	Med	SD	CV	P_{10}	P_{90}	Med	SD	CV	P_{10}	P_{90}	Med	SD	CV
Ri-no	0.41	14.5	2.4	35.0	4.4	0.53	4.8	3.2	1.7	0.6	0.61	7.0	2.7	2.4	0.8
Ri-PC	0.37	10.2	2.1	28.2	4.5	0.35	2.3	1.0	0.7	0.6	0.48	6.2	1.4	2.0	1.0
Ri-W	0.24	5.2	1.1	10.8	3.9	0.12	0.9	0.4	0.4	0.8	0.12	2.9	0.9	1.0	0.9
Ri-Y	0.32	6.1	1.7	11.5	3.2	0.32	1.5	0.6	0.4	0.6	0.35	2.9	1.1	0.9	0.7
Ri-EA	0.04	2.9	0.6	8.4	4.5	0.09	1.5	0.2	0.6	1.0	0.07	1.5	0.3	0.6	1.0
Ri-RR	0.16	3.9	0.9	14.1	4.9	0.33	2.9	1.5	1.0	0.7	0.34	2.9	1.0	1.1	0.8
P-Y	2.23	59.1	10.2	94.1	3.2	1.42	10.7	3.2	3.7	0.9	1.63	27.3	7.0	9.6	1.0

[a] P_{10} and P_{90} are the 10th and the 90th percentile of the data. Med is the median, SD is the standard deviation, and CV is the coefficient of variation.

data set. The values of $(f_0/f_{tot})^{0.5}$ did not significantly increase with flow depth. This might be because of the differences between the effects of steps in nature and those observed in laboratory experiments, where steps are perfectly shaped width-spanning elements. In nature, steps are typically arranged in more three-dimensional patterns, possibly resulting in different energy dissipation than would be observed in a simplified flume set-up.

[57] The stress partitioning approach of *Yager* [2006], combination Ri-Y, predicted values of $(f_0/f_{tot})^{0.5}$ similar to combination Ri-RR over a large range of relative flow depth, especially for streams with high boulder concentrations or large step slopes. Combination Ri-Y resulted in a median V_{pred}/V_{meas} value of 1.1 for the whole data set with a small coefficient of variation of 0.9, and 93% of the events were predicted within half an order of magnitude of the observed bedload volumes. When *Yager*'s [2006] approach was combined with the *Parker* [1990] bedload equation, combination P-Y, predicted bedload volumes were on average sevenfold larger than predicted with Ri-Y.

[58] The approach of *Rickenmann and Recking* [2011], combination Ri-RR, yielded consistently relatively good bedload predictions over a wide range of relative flow depths, with a median value of $V_{pred}/V_{meas} = 1.0$ for the whole data set and a small coefficient of variation of 1.1. The approach produced a comparatively good prediction accuracy especially for the long-term data, where a wide range of relative flow depths occurs.

[59] However, no individual equation performed best across the full range of channel types and the specific macro-roughness elements, i.e., no specific equation yielded consistently good predictions for each single event in a step-pool system or in a boulder bed stream. However, for streams with high boulder concentrations the approaches Ri-PC, Ri-W, and Ri-Y usually gave accurate predictions of bedload volumes, i.e., they predicted 90% of the events to

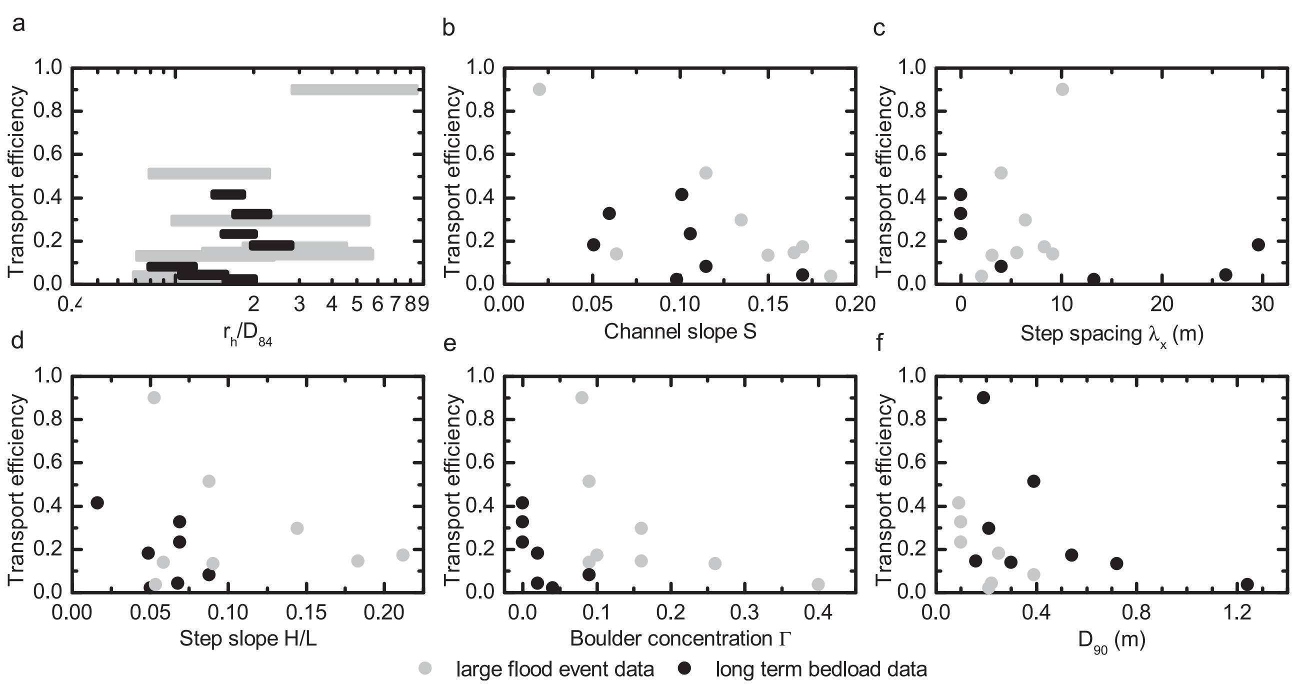

Figure 8. The transport efficiency in relation to the roughness measures. One point refers to the summed data of one stream. The floating bars in Figure 8a refer to the observed r_h/D_{84} range above the critical discharge Q_c. Transport efficiency TE is here defined as $TE = \Sigma V_{meas}/(1.5\Sigma[Q - Q_c]S^{1.5})$.

Table 7. Kendall Tau Rank Correlation Coefficient for the Relationship Between Transport Efficiency and Roughness Measures

	Channel Slope S	Step Spacing λ_x	Step Slope H/L	Boulder Concentration Γ	Grain Size D_{90}
Long-term data	−0.24	−0.51	−0.10	−0.69	−0.49
Event data	−0.50	0.43	0.00	−0.67	−0.50
All data	−0.36	−0.15	0.05	−0.27	−0.37

within a factor of 3 of the observed bedload volumes. This represents a significant improvement in prediction accuracy compared to the reference equation Ri-no.

[60] Interestingly, the purely empirical approach Ri-RR, which does not explicitly account for any specific type of macro-roughness element, estimated energy losses (i.e., values of $[f_0/f_{tot}]^{0.5}$) that resulted in relatively accurate bedload predictions. This suggests that either the physically based approaches in steep streams may still be insufficient in predicting the influence of macro-roughness on total flow resistance, or that the streambed characteristics and flow conditions in these streams cannot be assessed accurately enough when measuring the necessary parameters in the field. Furthermore, flow resistance partitioning for shallow flows in steep streams is not straightforward [*Rickenmann and Recking*, 2011]. *Zimmermann* [2010] concluded that it is difficult to distinguish between grain and form resistance for such flow conditions. Even though the flow resistance partitioning concept has been questioned in various studies [e.g., *David et al.*, 2011; *Wilcox et al.*, 2006; *Wilcox and Wohl*, 2006], its application was shown to result in bedload transport predictions that were up to an order of magnitude closer to observed transport rates than predictions from equations that did not account for additional flow resistance effects. The relatively good performance of the stress partitioning approach of *Yager* [2006] for streams with higher boulder concentrations indicates that this physically based correction for additional flow resistance is a step forward in better characterizing such stream conditions from a theoretical point of view. The improved bedload predictions support our assumption that physical roughness measures could consequently have a direct influence on bedload predictions. Moreover, our data showed relationships between macro-roughness in a stream and its transport efficiency (Figure 8, Table 7). For the range of investigated channel and flow conditions, the most significant correlations were observed between transport efficiency and boulder concentration, and between transport efficiency and the characteristic grain size D_{90} (Table 7). Transport efficiency, *TE*, is a ratio equivalent to an ideal dimensionless prefactor in the simple bedload equation (23) (with no accounting for macro-roughness), defined here by $TE = \Sigma V_{\mathrm{meas}}/(1.5\Sigma[Q - Q_c]S^{1.5})$, with Q = stream discharge.

5.3. Uncertainty of Roughness Parameter Estimation

[61] The flow resistance partitioning approaches presented here are based on measurements of channel parameters in flume experiments, often with simple geometric arrangements of roughness elements. Transferring the definitions of these roughness measures to the field situation is not straightforward, and parameter identification and measurement in the field may introduce some uncertainty for the flow-resistance partitioning calculations. Morphologic features such as step-pool sequences are not unambiguously identifiable and are subject to variable definitions [e.g., *Zimmermann et al.*, 2008]. The natural conditions in a mountain stream complicate measurements when rough water or dense vegetation makes field work difficult.

[62] One important measure, which was incorporated in three of the presented flow-resistance partitioning approaches, was the mean boulder diameter D_b. This parameter depends on the choice of a minimum diameter D_c, which a grain must possess to be regarded as a boulder or immobile grain. Since D_c is mainly controlled by flow conditions, an optimal definition for field measurements is challenging. For a specific flow D_c could be estimated using an equation for the initiation of bedload motion [e.g., *Bathurst et al.*, 1987; *Lamb et al.*, 2008]. But to prevent problems in comparing different streams, D_c should be defined as the grain size that is moved at a flow magnitude of a specific reoccurrence interval. Since we do not have the necessary information on the frequency of boulder motions, we made the most practical assumption and fixed D_c at 0.5 m. Moreover, this assumption allowed more robust data acquisition in the field, where measuring grains below a certain size is either uncertain, or requires very costly or time-demanding investigations.

[63] Whatever definition for D_c is used, uncertainty in the latter affects the roughness parameters of the flow resistance equations (Table 8) and consequently affects bedload predictions (Figure 9). As an example, for the Gamsa river, a 40% and 80% increase of D_c increased the mean boulder size, because smaller grains were not counted as boulders (Table 8). Boulder concentration slightly decreased and boulder step spacing became larger. The changed parameters lead to increased bedload transport rates in the approaches of *Yager* [2006] (Ri-Y) and *Pagliara and Chiavaccini* [2006] (Ri-PC) (Figures 9a and 9b) and also in the equation combination Parker-Yager (P-Y). The larger transport rates resulted in larger total bedload volumes for the example of the Gamsa stream event. Bedload volumes were

Table 8. Variation of Roughness Parameters With the Critical Grain Immobile Diameter D_c[a]

	$D_c = 0.5$ m	$D_c = 0.7$ m	$D_c = 0.9$ m
Number of boulders N	150	140	109
Mean boulder diameter D_b (m)	1.164	1.199	1.304
Boulder concentration Γ	0.164	0.163	0.150
Boulder step spacing λ_x (m)	5.57	5.94	7.01
Height of sediment z_m[b] (m)	0.561	0.585	0.671
Boulder protrusion p_u (m)	0.602	0.614	0.633
Block concentration α	0.205	0.204	0.188

[a]Table data is from the Gamsa stream.
[b]Height of sediment above the base of immobile grains.

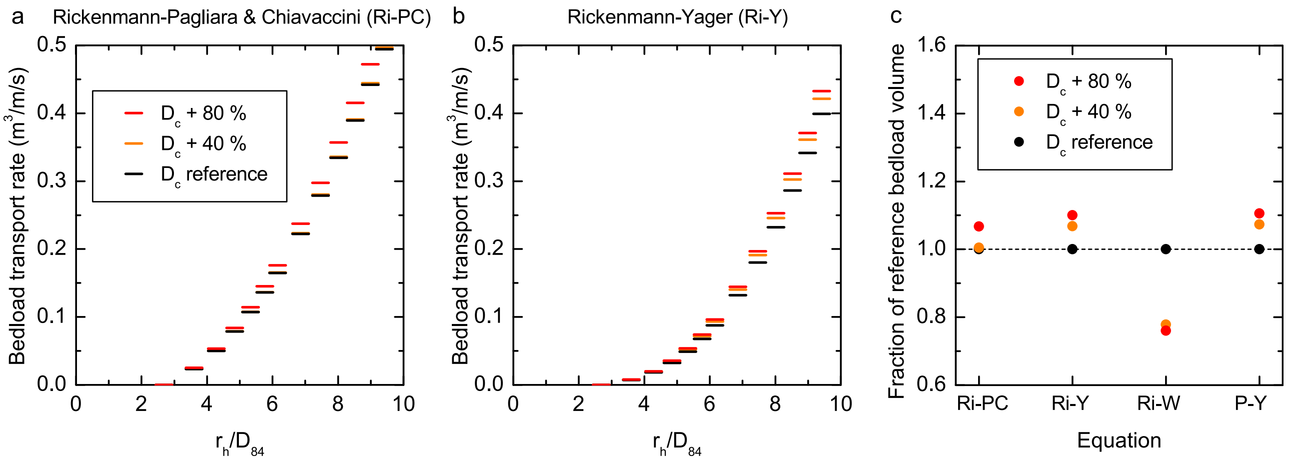

Figure 9. (a and b) The sensitivity of the bedload transport rate per unit width and (c) bedload event volumes to variation of the critical immobile grain size D_c. Data is from the Gamsa stream. The stress partitioning equations are defined in Table 4.

up to 11% larger than in calculations with the reference critical diameter D_c (Figure 9c). The increase of D_c had an inverse effect on the predictions with the approach of *Whittaker et al.* [1988] (Ri-W): bedload volumes were reduced by up to 24% (Figure 9c). This contrasting effect is due to the dominant influence of D_b in relation to the block concentration α in the flow resistance calculation of *Whittaker et al.* [1988].

[64] In small streams shear stresses at high flows can get competent to move boulders that are larger than 0.5 m in diameter [*Turowski et al.*, 2009]. When all grain sizes (including boulders) are mobile at high flow, the validity of the approaches using boulder concentration is in question. This is because the sensitive parameter boulder concentration should theoretically become zero and therefore the predicted additional flow resistance should also equal zero. A further uncertainty in predicting bedload volumes is the variability in threshold discharge for the onset of transport. There have been few attempts to relate discharge and initiation of bedload transport on the basis of field data from steep streams [*Bathurst et al.*, 1987; *Lamb et al.*, 2008; *Turowski et al.*, 2011]. However, for large floods the influence of transport thresholds on predicted bedload transport rates is smaller than for small flood events, because flows are much higher than the threshold flow.

6. Conclusions

[65] Bedload transport and flow resistance equations were combined to account for flow resistance because of macro-roughness elements and shallow flows in steep streams. Several flow-resistance partitioning methods were used to estimate a reduced energy slope as a basis for modified bedload transport calculations. This procedure significantly reduced the overprediction of observed bedload volumes, as compared to the predictions with the reference transport equation of *Rickenmann* [2001] that did not account for macro-roughness effects.

[66] The tested approaches yielded highly variable improvements in bedload transport prediction accuracy, mainly depending on the size and density of macro-roughness elements and on the flow conditions. The approaches that account for the effects of large boulders generally performed better in streams featuring a high boulder concentration or a step-pool system. For rough channels with a high boulder concentration, the transport equation of *Rickenmann* [2001] combined with the flow resistance equations of *Pagliara and Chiavaccini* [2006], *Yager* [2006], and *Whittaker et al.* [1988] predicted at least 75% of the events to within a factor of 3 of the observed values. The approach by *Egashira and Ashida* [1991], which estimates flow resistance by a measure of step-pool geometry, did not improve bedload predictions compared to the reference equation.

[67] For practical applications, if no detailed roughness information is available for a given stream, the approach of *Rickenmann and Recking* [2011] represents a simple way to account for additional flow resistance in steep streams with small, relative flow depths. The approach generated the best average performance for all study streams, including a large range of streambed characteristics and flow conditions. This suggests either that the more physically based approaches in steep streams may still be insufficient in predicting the influence of macro-roughness on total flow resistance, or that the identification and measurement of macro-roughness and flow conditions in these streams are not accurate enough. The results indicate that the physically based approaches may not apply to the wide range of streambed and flow conditions represented by the study streams. However, the approaches that take into account a measure of macro-roughness resulted in bedload transport predictions that were up to an order of magnitude closer to observed transport rates than predictions from equations that did not account for additional flow resistance effects. The relatively good performance of the stress partitioning approach of *Yager* [2006] for streams with higher boulder concentrations indicates that this physically based correction for additional flow resistance is a step forward in better characterizing such stream conditions from a theoretical point of view.

[68] **Acknowledgments.** This study was supported by the Swiss Federal Office for the Environment (contract no. 06.0083.PJ/G063-0651). Additional support to D.R. and J.M.T. was obtained through SNF grant

200021_124634/1. The authors thank Fabian Blaser and Michael Pauli for field assistance, Angela Klaiber for assistance in data compilation, and Ingo Völksch for programming support. We thank Rob Ferguson and two anonymous reviewers for their constructive comments that improved the paper.

References

Abgottspon, E., J. Seiler, B. Zarn, and M. Zimmermann (2001), Hochwasser vom Oktober 2000 in der Lonza: Temporäre schutzmassnahmen verhindern millionenschäden, *Wasser Energie Luft*, *93*(3/4), 87–92.

Abrahams, A. D., and P. Gao (2006), A bed-load transport model for rough turbulent open-channel flows on plane beds, *Earth Surf. Processes Landforms*, *31*, 910–928, doi:10.1002/esp.1300.

Badoux, A., and D. Rickenmann (2008), Berechnungen zum Geschiebetransport während der Hochwasser 1993 und 2000 im Wallis, *Wasser Energie Luft*, *2008*(3), 217–227.

Bänziger, R., and H. Burch (1990), Acoustic sensors (hydrophones) as indicators for bed load transport in a mountain torrent, paper presented at Hydrology in Mountainous Regions. I—Hydrological Measurements; the Water Cycle, Lausanne, Switzerland.

Bathurst, J. C. (1978), Flow resistance of large-scale roughness, *J. Hydraul. Eng.*, *104*(12), 1587–1603.

Bathurst, J. C. (1985), Flow resistance estimation in mountain rivers, *J. Hydraul. Eng.*, *111*(4), 625–643.

Bathurst, J. C. (2002), At-a-site variation and minimum flow resistance for mountain rivers, *J. Hydrol. Eng.*, *269*, 11–26.

Bathurst, J. C., R.-M. Li, and D. B. Simons (1981), Resistance equation for large-scale roughness, *J. Hydraul. Eng.*, *107*, 1593–1613.

Bathurst, J. C., W. H. Graf, and H. H. Cao (1987), Bed load discharge equations for steep mountain rivers, in *SedimentTtransport in Gravel-bed Rivers*, edited by C. R. Thorne, et al., pp. 453–477, John Wiley, New York.

Bezzola, G. R., and C. Hegg (Eds.) (2007), *Ereignisanalyse Hochwasser. (2005), Teil 1—Prozesse, Schäden und erste Einordnung*, 215 pp., BAFU and WSL, Bern, Switzerland.

Bezzola, G. R., and C. Hegg (Eds.) (2008), *Ereignisanalyse Hochwasser 2005, Teil 2—Analyse von Prozessen, Massnahmen und Gefahrengrundlagen*, 427 pp., Bern, Switzerland.

Burkhard, A., and M. N. R. Jäggi (2003), Hochwasserschutz im Wallis, Massnahmen an der Saltina, *Wasser Energie Luft*, *95*(9/10), 273–280.

BWG (2002), *Hochwasser 2000—Les crues* 2000, 248 pp., Bundesamt für Wasser und Geologie BWG, Bern, Switzerland.

Canovaro, F., and L. Solari (2007), Dissipative analogies between a schematic macroroughness arrangement and step–pool morphology, *Earth Surf. Processes Landforms*, *32*, 1628–1640.

Canovaro, F., E. Paris, and L. Solari (2007), Effects of macro-scale bed roughness geometry on flow resistance, *Water Resour. Res.*, *43*, W10414, doi:10.1029/2006WR005727.

Carson, M. A., and G. A. Griffiths (1987), Bedload transport in gravel channels, *J. Hydrol.*, New Zealand, *26*(1), 151, special issue.

Chiari, M. (2008), Numerical modelling of bedload transport in torrents and mountain streams, Doctoral thesis, University of Natural Resources and Applied Life Sciences, Vienna, Austria.

Chiari, M., and D. Rickenmann (2011), Back-calculation of bedload transport in steep channels with a numerical model, *Earth Surf. Processes Landforms*, *36*(6), 805–815, doi:10.1002/esp.2108.

Chiari, M., K. Friedl, and D. Rickenmann (2010), A one-dimensional bedload transport model for steep slopes, *J. Hydraul. Res.*, *48*(2), 152–160, doi:10.1080/00221681003704087.

Church, M., and A. Zimmermann (2007), Form and stability of step-pool channels: Research progress, *Water Resour. Res.*, *43*(3), W03415, doi:10.1029/2006WR005037.

Comiti, F., D. Cadol, and E. Wohl (2009), Flow regimes, bed morphology, and flow resistance in self-formed step-pool channels, *Water Resour. Res.*, *45*(4), W04424, doi:10.1029/2008WR007259.

D'Agostino, V., and M. A. Lenzi (1999), Bedload transport in the instrumented catchment of the Rio Cordon Part II: Analysis of the bedload rate, *Catena*, *36*(3), 191–204.

David, G. C. L., E. Wohl, S. E. Yochum, and B. P. Bledsoe (2010), Controls on spatial variations in flow resistance along steep mountain streams, *Water Resour. Res.*, *46*(3), W03513, doi:10.1029/2009WR008134.

David, G. C. L., E. E. Wohl, S. E. Yochum, and B. P. Bledsoe (2011), Comparative analysis of bed resistance partitioning in high gradient streams, *Water Resour. Res.*, WR7507, doi:10.1029/2010WR009540.

Egashira, S., and K. Ashida (1991), Flow resistance and sediment transportation in streams with step-pool bed morphology, in *Fluvial Hydraulics of Mountain Regions*, edited by A. Armanini et al., pp. 45–58, Springer, Heidelberg, Germany.

Einstein, H. A., and R. B. Banks (1950), Fluid Resistance of Composite Roughness, Eos. *Trans. AGUnion*, *31*(4), 603–611.

Fehr, R. (1987), Einfache Bestimmung der Korngrössenverteilung von Geschiebematerial, *Schweizer Ingenieur und Architekt*, *105*(38), 1004–1109.

Ferguson, R. (2007), Flow resistance equations for gravel- and boulder-bed streams, *Water Resour. Res.*, *43*(12), W05427, doi:10.1029/2006WR005422.

geo7 (1998), Ortsplanungsrevision Matten, St. Stephan: Gefahrenbeurteilung, Gefahrenkarte und Massnahmenkonzept für den Mattenbach, Ereignisdokumentation.

Gomez, B., and M. Church (1989), An assessment of bed-load sediment transport formulas for gravel bed rivers, *Water Resour. Res.*, *25*(6), 1161–1186, doi:10.1029/WR025i006p01161.

Govers, G., and G. Rauws (1986), Transporting capacity of overland flow on plane and on irregular beds. *Earth Surf. Processes Landforms*, *11*, 515–524.

Hegg, C., B. W. McArdell, and A. Badoux (2006), One hundred years of mountain hydrology in Switzerland by the WSL, *Hydrol. Processes*, *20*, 371–376.

Hey, R. D. (1979), Flow Resistance in Gravel-Bed Rivers, *J. Hydraul. Eng.*, *105*(4), 365–379.

Hilker, N., A. Badoux, and C. Hegg (2009), The Swiss flood and landslide damage database 1972-2007, *Nat. Hazards Earth Syst. Sci.*, *9*(3), 913–925.

Jäggi, M. N. R., U. Nigg, and P. Teysseire (2004), Die Sedimentkatastrophe von Baltschieder, paper presented at Interpraevent 2004, Riva del Garda.

Jarrett, R. D. (1984), Hydraulics of high-gradient streams, *J. Hydraul. Eng.*, *110*(11), 1519–1539.

Julien, P. Y. (2002), *River Mechanics*, 434 pp., Cambridge Univ. Press, New York.

Katul, G., P. Wiberg, J. Albertson, and G. Hornberger (2002), A mixing layer theory for flow resistance in shallow streams, *Water Resour. Res.*, *38*(11), 1250, doi:10.1029/2001WR000817.

Keulegan, G. H. (1938), Laws of turbulent flow in open channels, *J. Res. Nat. Bur. Stand.*, *21*(6), 707–741.

Kirchhofer, W., and B. Sevruk (1992), Mean annual corrected precipitation depths 1951–1980, in *Hydrological Atlas of Switzerland*, Plate 2.2, Swiss Federal Office for the Environment, Bern.

Lamarre, H., and A. G. Roy (2008), A field experiment on the development of sedimentary structures in a gravel-bed river, *Earth Surf. Processes Landforms*, *33*, 1064–1081.

Lamb, M. P., W. E. Dietrich, and J. G. Venditti (2008), Is the critical Shields stress for incipient sediment motion dependent on channel-bed slope?, *J. Geophys. Res.*, *113*(F2), 20, F02008, doi:10.1029/2007jf000831.

LCH-EPFL (2003), Hochwasserschutzprojekt der Gamsa in Gamsen (Brig-Glis). Hydraulische Modellversuche. Schlussbericht, EPFL, Lausanne, Switzerland.

Lenzi, M. A., V. D'Agostino, and P. Billi (1999), Bedload transport in the instrumented catchment of the Rio Cordon Part I: Analysis of bedload records, conditions and threshold of bedload entrainment, *Catena*, *36*(3), 171–190.

Manga, M., and J. W. Kirchner (2000), Stress partitioning in streams by large woody debris, *Water Resour. Res.*, *36*(8), 2373–2379, doi:10.1029/2000WR900153.

Meyer-Peter, E., and R. Müller (1948), Formulas for bedload transport, paper presented at 2nd meeting Int. Assoc. Hydraulic Structures Res., Stockholm, Sweden.

Millar, R. G. (1999), Grain and form resistance in gravel-bed rivers, *J. Hydraul. Res.*, *37*(3), 303–312.

Millar, R. G., and M. C. Quick (1994), Flow resistance of high-gradient gravel channels in *Hydraulic Engineering '94*, edited by G. V. Cotroneo and R. R. Rumer, pp. 717–721, ASCE, New York.

Montgomery, D. R., and J. M. Buffington (1997), Channel-reach morphology in mountain drainage basins, *GSA Bulletin*, *109*(5), 596–611.

Nelson, J. M., S. R. McLean, and S. R. Wolfe (1993), Mean flow and turbulence fields over two-dimensional bed forms, *Water Resour. Res.*, *29*(12), 3935–3953, doi:10.1029/93WR01932.

Oeko-B AG (2006), Ereigniskataster Nidwalden, Unwetter August 2005, Oeko-B AG & Niederer + Pozzi Umwelt AG.

Pagliara, S. (2008), Closure to "flow resistance of rock chutes with protruding boulders" by S. Pagliara and P. Chiavaccini, *J. Hydraul. Eng.*, *134*(7), 1022–1023.

Pagliara, S., and P. Chiavaccini (2006), Flow resistance of rock chutes with protruding boulders, *J. Hydraul. Eng.*, *132*(6), 545–552.

Palt, S. M. (2001), Sedimenttransportprozesse im Himalaya-Karakorum und ihre Bedeutung für Wasserkraftanlagen, Doctoral thesis, Universität Karlsruhe, Karlsruhe.

Papanicolaou, A. N., A. Bdour, and E. Wicklein (2004), One-dimensional hydrodynamic/sediment transport model applicable to steep mountain streams, *J. Hydraul. Res.*, *42*(4), 357–375.

Parker, G. (1990), Surface-based bedload transport relation for gravel rivers, *J. Hydraul. Res.*, *28*(4), 417–436.

Parker, G., and A. W. Peterson (1980), Bar resistance of gravel-bed streams, *J. Hydraul. Div.*, *106*(10), 1559–1573.

Recking, A., P. Frey, A. Paquier, P. Belleudy, and J. Y. Champagne (2008), Feedback between bed load transport and flow resistance in gravel and cobble bed rivers, *Water Resour. Res.*, *44*, W05412, doi:10.1029/2007WR006219.

Rickenmann, D. (1991), Hyperconcentrated flow and sediment transport at steep flow, *J. Hydraul. Eng.*, *117*(11), 1419–1439, doi:10.1061/(ASCE)0733-9429(1991)117:11(1419).

Rickenmann, D. (1994), An alternative equation for the mean velocity in gravel-bed rivers and mountain torrents, paper presented at Hydraulic Engineering ’94, American Society of Civil Engineers, Buffalo, NY.

Rickenmann, D. (1996), Fliessgeschwindigkeit in Wildbächen und Gebirgsflüssen, *Wasser, Energie, Luft*, *88*(11/12), 298–304.

Rickenmann, D. (1997), Sediment Transport in Swiss Torrents, *Earth Surf. Processes Landforms*, *22*, 937–951.

Rickenmann, D. (2001), Comparison of bed load transport in torrents and gravel bed streams, *Water Resour. Res.*, *37*(12), 3295–3305, doi:10.1029/2001WR000319.

Rickenmann, D. (2005), Geschiebetransport bei steilen Gefällen, in *Festkolloquium*, edited, Versuchsanstalt für Wasserbau, Hydrologie und Glaziologie.

Rickenmann, D., and A. Koschni (2010), Sediment loads due to fluvial transport and debris flows during the 2005 flood events in Switzerland, *Hydrol. Processes*, *24*(8), 993–1007, doi:10.1002/hyp.7536.

Rickenmann, D., and B. W. McArdell (2007), Continuous measurement of sediment transport in the Erlenbach stream using piezoelectric bedload impact sensors., *Earth Surf. Processes Landforms*, *32*, 1362–1378.

Rickenmann, D., and A. Recking (2011), Evaluation of flow resistance in gravel-bed streams through a large field data set, *Water Resour. Res.*, W07538, doi:10.1029/2010WR009793.

Rickenmann, D., M. Chiari, and K. Friedl (2006), SETRAC—A sediment routing model for steep torrent channels, paper presented at River Flow 2006, Taylor & Francis, London, UK.

Schoklitsch, A. (1962), *Handbuch des Wasserbaus (in German)*, 3rd ed., Springer, Vienna, Austria.

Smart, G. M., and M. N. R. Jaeggi (1983), Sediment transport on steep slopes, pp. 89–191, Versuchsanstalt für Wasserbau, Hydrologie und Glaziologie, Eidgenössische Technische Hochschule Zürich, Zürich, Switzerland.

Smart, G. M., M. J. Duncan, and J. M. Walsh (2002), Relatively rough flow resistance equations, *J. Hydraul. Eng.*, *128*(6), 568–578.

Turowski, J. M., E. M. Yager, A. Badoux, D. Rickenmann, and P. Molnar (2009), The impact of exceptional events on erosion, bedload transport and channel stability in a step-pool channel, *Earth Surf. Processes Landforms*, *34*, 1661–1673.

Turowski, J. M., A. Badoux, and D. Rickenmann (2011), Start and end of bedload transport in gravel-bed streams, *Geophys. Res. Lett.*, *38*(4), L04401, doi:10.1029/2010GL046558.

USACE (2000), Hydrologic Modeling System HEC-HMS - Technical Reference Manual, edited by Engineers, U. A. C. o., US Army Corps of Engineers, Davis, California.

Weingartner, R., and H. Aschwanden (1992), Discharge Regime—the basis for estimation of average flows, in *Hydrological Atlas of Switzerland*, Plate 5.2, Swiss Federal Office for the Environment, Bern, Switzerland.

Whittaker, J. G. (1986), An equation for predicting bedload transport in steep mountain step-pool stream, in *9th Australasian Fluid Mechanics Conference*, edited, Auckland.

Whittaker, J. G., and M. N. R. Jaeggi (1982), Origin of step-pool systems in mountain streams, *J. Hydraul. Div.*, *108*(6), 758–773.

Whittaker, J. G., W. E. Hickman, and R. N. Croad (1988), Riverbed Stabilisation with Placed Blocks, Central Laboratories, Works and Development Corporation, Lower Hutt, NZ.

Wilcox, A. C., and E. E. Wohl (2006), Flow resistance dynamics in step-pool stream channels: 1. Large woody debris and controls on total resistance, *Water Resour. Res.*, *42*(5), W05418, doi:10.1029/2005WR004277.

Wilcox, A. C., J. M. Nelson, and E. E. Wohl (2006), Flow resistance dynamics in step-pool channels: 2. Partitioning between grain, spill, and woody debris resistance, *Water Resour. Res.*, *42*, W05419, doi:10.1029/2005WR004278.

Wohl, E. E., and D. M. Thompson (2000), Velocity characteristics along a small step-pool channel, *Earth Surf. Processes Landforms*, *25*(4), 353–367.

Yager, E. M. (2006), Prediction of sediment transport in steep, rough streams, PhD thesis, 232 pp., University of California, Berkeley, California.

Yager, E. M., J. W. Kirchner, and W. E. Dietrich (2007), Calculating bed load transport in steep boulder bed channels, *Water Resour. Res.*, *43*, W07418, doi:10.1029/2006WR005432.

Zeller, J. (1985), Feststoffmessung in kleinen Gebirgseinzugsgebieten, *Wasser Energie Luft*, *77*(7/8), 246–251.

Zimmermann, A. (2010), Flow resistance in steep streams: An experimental study, *Water Resour. Res.*, *46*, W09536, doi:10.1029/2009WR007913.

Zimmermann, A. E., M. Church, and M. A. Hassan (2008), Identification of steps and pools from stream longitudinal profile data, *Geomorphology*, *102*, 395–406.

A. Badoux, J. W. Kirchner, M. Nitsche, D. Rickenmann, and J. M. Turowski, Mountain Hydrology and Torrents Unit, WSL Swiss Federal Institute for Forest, and Avalanche Research SLF, Zürcherstr. 111, 8903 Birmensdorf, Switzerland. (nitsche@wsl.ch)